

BRITISH GEOLOGICAL SURVEY
Natural Environment Research Council

TECHNICAL REPORT WN/91/18

WN/91/18

**A RECONNAISSANCE MT SURVEY
ACROSS THE AE FOREST-SOUTHERN UPLANDS
INITIAL REPORT**

D. Beamish and D.G. Wallis

Bibliographic reference

**Beamish, D. and Wallis, D.G., A
reconnaissance MT survey across the Ae
forest - Southern Uplands : Initial Report
British Geological Survey, Technical
Report, WN/91/18**

This report has been generated from a scanned image of the document with any blank pages removed at the scanning stage.
Please be aware that the pagination and scales of diagrams or maps in the resulting report may not appear as in the original

INTRODUCTION

This report describes a reconnaissance MagnetoTelluric (MT) survey carried out as part of the Southern Upland mapping programme. The 8 site survey, along a 14 km NW-SE profile, was centred on the Ae forest area to the east of Thornhill and to the SW of Moffat. The measurements were undertaken across one of the fault-bounded tract sequences of greywackes in the Central Belt. The purpose of the limited survey is to investigate the possibility of 'locally' detecting concealed tectonostratigraphic structure by virtue of its (possible) resistivity expression.

For those unfamiliar with MT, the technique is described in the newer editions of standard text-books on geophysical methods such as Dobrin and Savit (1988). The MT method attempts to provide a resistivity cross-section, often through the whole crust. The sensors currently available restrict information to depths greater than several hundred metres. The present survey was carried out using a new 7-channel field instrument developed in-house by the BGS.

The present *initial* report provides detailed information on the survey, the measurements undertaken and the data obtained. A limited appraisal of the geoelectric structure is then carried out. The results presented are incomplete and are intended as a rapid 'turn-around' of the field measurements.

SURVEY PURPOSE.

The profile MT survey was conducted in September 1991 and was centered on the Ae forest area to the east of Thornhill and to the SW of Moffat (Sheet 78, 1:50000 O.S.). The survey profile obtained (Figures 1, 2 & 3) was very much in accord with the 'target' cross-section which was established through discussions with land-survey colleagues in Murchison House and on the basis of regional-scale geophysical anomaly maps.

The purpose of the MT survey was to carry out reconnaissance MT measurements across one of the fault-bounded tract sequences of greywackes within the Southern Upland succession (Stone *et al*, 1987). The measurements were centred on the Queensberry formation as shown in Figure 1. In a more regional context the purpose of the survey was to investigate the possibility of 'locally' detecting the geoelectric (resistivity) expression of a tectonic feature identified on regional geomagnetic variation anomaly maps (Banks *et al*, 1983) and on regional magnetic anomaly maps (Kimbell, 1991). According to Kimbell (1991) a long wavelength magnetic high in the survey region is attributed to magnetisation contrasts at mid to lower crustal depths. The inferred source is a block of magnetic crust bounded (i) to the south by the reflective/conductive boundary (geophysical Iapetus Suture), (ii) to the north by the Orlock Bridge - Kingledores Fault and (ii) to the east by the Moffat Valley lineament. In geoelectric terms the profile crosses the 'zero line' (i.e. conductive centre-of-gravity) of the Southern Uplands geoelectric anomaly which has been mapped (albeit loosely) across the whole of southern Scotland (Figure 2).

A subsidiary (technical) purpose behind the survey was to 'field-test' the performance of the new

MT instrumentation which was developed in-house during the summer of 1991. A consequence of this secondary requirement was that the quality control of the data acquired was very limited (due to in-field time constraints).

SURVEY DESCRIPTION.

Field logistics resulted in about one sounding per day (24 hours) over the 7 day survey. By performing two short duration (day-only) soundings, eight sites were occupied with details as given in Table 1. The profile, shown in Figure 3, is about 14 km long. The northern-most site 001 is north of the forest and on Mitchellsacks farm land which abuts the southern escarpment of the Lowther Hills. Sites 002-006 are all on Forestry Commission land and were undertaken in clearings. The forest itself was too dense for sensible installation of cables and sensors. The clearings, usually with a high degree of forest debris, were found to be 'difficult' in terms of site installation. Sites 007 and 008 are to the south of the forest and on land belonging to Meikleholm and Cumleys farms respectively.

Survey procedure involved site uplift (about 1.5 hours), redeployment and installation (about 2 to 3 hours) followed by test measurements to verify sensors and test noise levels. The new instrumentation acquires data in two frequency bands. High-band recording refers to the frequency interval from 0.5 to 250 Hz with 7-channel data being sampled at 500 Hz. Low-band recording refers to the frequency interval from 0.005 to 2.5 Hz with data being sampled at 5 Hz. High-band recording was always undertaken first. When subsequent low-band measurements were underway, further site selection and permissions were carried out. Low-band sounding continued overnight, except at two sites (001 and 008), by leaving the Land-Rover and generator on-site. Data backups were undertaken each evening. The survey produced some 50 Mbytes of raw sounding data.

QUALITY CONTROL

The performance of the new instrumentation will be discussed at a technical level elsewhere. A large number of technical matters influenced the quality of the 7-channel measurements obtained during the survey. Some of the main contributors to data quality should be pointed out since they have a bearing on data interpretation. As shown in Table 1, the field survey was conducted using site codes (111-888). These site codes, in chronological survey order, are used to provide comments.

Measurements at the first two sites (111 and 222) were undertaken while attempting to solve a 'ground-loop' noise problem. The identification of this problem was complicated by the use of a borrowed generator whose output voltage was set high and was delivering a frequency close to 60 Hz. The main ground loop problem was effectively solved by the installation of site 333 (further

'unpressured' tests are required though). During operation of the first two sites the performance of the gain stages on the new E-field sensors were also being evaluated.

The data at site 333 should be considered 'representative' of the data quality that the new instrument can provide when self-inflicted and environmental quality-degrading factors are at a minimum. In order to operate at site 444, we had to request that the electric fence at Mitchellsacks farm be turned off. Site 444 was a short duration sounding since the field was required for sheep. A short duration sounding essentially means that the low-band (frequencies below 1 Hz) data quality will be low.

The prevailing (stable) weather system had deteriorated to gusting wind and rain by site 555. A 'Friday the 13'th' virus appeared on the borrowed IBM-PC used for the survey. The virus, although alarming, was found to be operationally unharmed if the system clock date was left unset. During the overnight recording the local magnetic centre-box filled with water (rubber-seal left loose) and low-band data were degraded.

The 24 hour measurements at site 666 were unhampered by obvious sources of noise. By site 777 the majority of external cabling was water soaked and we began to experience contact problems, particularly in the magnetic sensor cabling. In the absence of an air-gun heater, attempts to 'dry-out' the equipment were only partially successful and the overnight low-band recording was of poor quality. In order to operate at site 888 we had to request that the electric fence system at the adjacent farm of Gillrigg be turned off. Site 888 was a short duration (day-only) sounding.

Data acquisition and quality assessments were carried out on an 'old' borrowed IBM-PC operating at 5.9 MHz. Although adequate for purely acquisition aspects of the new instrument the processing power proved totally inadequate for even a moderate level of in-field processing and assessment of the data.

In summary *all* the high-band (frequencies greater than 1 Hz) measurements were of high quality but the low-band measurements were subjected to a variety of noise sources which degraded their quality. Most of the reasons for the quality downgrade have been identified and can be rectified. For the reasons discussed above, only field soundings 333 and 666 (sites 002 and 006) provided high quality data across the complete sounding bandwidth.

SOUNDING RESULTS

All the data collected have been routinely processed by a new robust remote reference algorithm installed on the Keyworth VAX. In addition to standard MT parameters, vertical field (tipper) measurements were obtained. Since the vertical fields measured were low, these data have still not been 'worked-up' and only the MT results are discussed here.

Sounding curves for all 8 sites are shown in the measured frame (XY and YX data) in Figure 4. The XY component of the sounding refers to the apparent resistivity and phase looking in the principal N-S direction and the YX component is the equivalent result in the E-W direction. Poor quality results (low predicted coherence) have been omitted and error bars are +/- one standard error. The overall high quality (small error bars) of the high band (frequencies above 1 Hz) results can be noted together with the site dependent variable quality of the low band results.

A brief comparison of the principal sounding results shown in Figure 4 reveals a broad set of common features across the profile together with site specific differences. In terms of differences, the two sites (007 and 008) to the south possess lower apparent resistivities at high frequencies. These sites lie within the upper Palaeozoic Lochmaben basin and are found to be influenced by the cover of conductive sandstones. Across the whole profile only site 005 appears to be influenced by static distortion which is a localised effect producing parallel offsets in the apparent resistivity data (the phase is unaffected). A major transition, in terms of the overall character of the soundings, takes place between sites 001 and 002.

Penetration depths.

The sounding curves in Figure 4 represent directional estimates of the resistivity structure from shallow depths (highest frequencies) down through the crustal section (decreasing frequencies). In order to provide a rough estimate of the effective depth of penetration across the survey profile we have calculated the c-response function using the average resistivity (a rotational invariant) obtained using the results shown in Figure 4. The real part of the complex c-response is a real length and provides a measure of the effective depth of penetration as a function of frequency.

The results for all 8 sites are shown together in Figure 5. Since site specific differences exist, different groups of symbols refer to different sounding characteristics across the profile. The results for site 001 are shown as open circles. The results for sites 002-006 are shown as solid stars and the results for sites 007 and 008 are shown as solid circles. The reasons for these characteristic groupings are evident in Figure 5 when both the real and imaginary parts of the c-response results are examined. Effective penetration depths, as a function of frequency, are obtained by examination of the real part of the c-response (left diagram of Fig. 5). At frequencies above 50 Hz, penetration depths are all less than 1 km. The shallowest depths of penetration are 100 to 200 metres at sites 007 and 008 and arise from the conductive sandstones above the greywacke formation. Apart from these two sites resistivity information on the upper kilometer of the section is contained in the results above about 20 Hz.

Apart from site 001, information on the resistivity section down to about 10 km is obtained in the soundings down to a frequency of about .3 Hz. The middle and lower crustal section is covered primarily at frequencies below .1 Hz. If the data were 1-D (resistivity varies only with depth) the real part of the c-response in Figure 5 would increase monotonically with decreasing frequency. The apparent turning point at the lowest frequencies in Figure 5 is due to the fact that the data are

not 1-D.

Dimensional characteristics.

An MT sounding is a tensor (directional) set of coupled measurements. The tensor theoretically provides information on the dimensionality of the geoelectric section being probed. In practice our ability to determine dimensional information is limited to one of *degree* rather than some absolute determination. Since the data will be modelled as a function of frequency, it is useful to construct a set of measures of the dimensional attributes of the soundings as a function of frequency. The dimensional weights (D1, D2 and D3) serve this purpose (Beamish, 1986) and are shown for each site in Figure 6 as a function of frequency. D1 refers to 1-D, D2 refers to 2-D and D3 refers to 3-D influences on the sounding data.

The dimensional characteristics shown in Figure 6 are frequency dependent. Using Figure 5 we estimate frequencies above 50 Hz correspond to penetration depths of less than 1 km, frequencies above 1 Hz correspond to depths of less than 3 km and frequencies less than .1 Hz correspond to penetration of the middle (> 10 km) and lower crust. Clearly over the whole bandwidth, the 1-D weights predominate but are found to decrease with decreasing frequency (greater penetration). This situation is normal. At a number of sites (e.g. site 006, Fig.6) the 1-D weights show a distinct decrease at the highest frequencies implying that the upper 1 km of the section provides a 'local' non 1-D contribution. Sites 007 and 008 display the most 1-D behaviour through the upper 10 km of the section. Site 001 shows the least 1-D type behaviour through the upper crustal section.

The transition to distinctly more 2-D behaviour is apparent at all sites with decreasing frequency. This behaviour implies a deep seated and regional geoelectric anisotropy. The largest contributions from the D3 (three dimensional) weights occur at very low frequencies at sites 001 and 002.

Geoelectric strike azimuths.

The MT tensor can be rotated (or decomposed) to provide a horizontal azimuth which corresponds to a direction of maximum (or minimum) resistivity. The azimuth, so obtained, is equivalent to the direction of geoelectric strike which is assumed 2-D. When the data are predominantly 1-D such azimuths may be indeterminate. The geoelectric strike directions for all 8 sites are shown in Figure 7 as a function of frequency. Azimuths refer to grid north (positive clockwise) and standard errors are shown. The azimuths obtained at site 005 are likely to be in error due to the static distortion encountered.

The most rapid movements in strike direction occur at the highest frequencies and, where accurate, indicate local structural influences on a scale less than the average site separation of

about 2 km. There is a degree of consistency in the azimuths obtained at mid-frequencies across the profile. These azimuths (+30 to +60 degrees) correspond to sectional penetration of the upper crustal basement. The most stable azimuths occur at the lowest frequencies where 2-D regional influence is a maximum. The azimuths obtained show a degree of progression across the profile and appear to be slightly different to the azimuths of the upper crustal basement. Below a frequency of 0.1 Hz the azimuth at site 001 remains frequency dependent but a greater degree of stability is observed at all other sites. At site 002 the low frequency azimuth is +45 degrees and is found to rotate to +50 to +60 degrees by sites 003 and 004. The site 005 data has not been corrected for static distortion. At sites 006, 007 and 008 the regional strike direction is between +60 and +70 degrees.

It is intended to carry out further summaries of the directions of geoelectric anisotropy when the vertical magnetic field data have been properly assessed.

Approximate 1-D inversion.

Although the data display 2-D characteristics, particularly with decreasing frequency, the formation of a rotational invariant such as the average resistivity can be useful for initial 1-D assessments of the vertical resistivity structure across the profile. The Niblett-Bostick transform, a fairly crude and approximate mapping of the data to an equivalent (1-D) resistivity profile, was applied to the average resistivity invariant data at each site. The transform results, with associated standard error bars, are shown in Figure 8. The presentation uses a log depth display between 100 and 100,000 metres on the left and a linear depth display between 0 and 10 km on the right. The left display, using log/log coordinates, is the 'natural resolution' scale of MT data. Although displayed for completeness, the data at site 005 have not been corrected for static distortion and will necessarily display an 'offset' in the resistivity profile.

Despite data gaps, and variable data quality at large penetration depths, the approximate 1-D results across the profile clearly indicate a major crustal dislocation (in resistivity structure) between sites 001 and 002. At sites 002 to 008, the results indicate a conductive mid to lower crustal profile with resistivities of the order of 100 ohm.m and less. At site 001, the equivalent resistivities are achieved by a depth of between 2 and 3 km.

Apart from site 001 upper crustal basement resistivities are fairly uniform across the profile, although some progression to the south of the dislocation is evident. At sites 002 and 003 apparent (1-D) basement resistivities are in the range 300 to 500 ohm.m while values of 500 to 900 ohm.m are observed to the south-east.

The approximate transforms shown in Figure 8 are not the best method of detecting layer interface behaviour in the vertical profile. The results of Figure 8 *suggest* that any resistivity contrasts between the greywacke sequence and electrical basement are likely to be small and may not be detectable except in a gradational sense. The behaviour of the high frequency data from sites 007

and 008 indicates that the sounding bandwidth is insufficient to directly detect the sandstone cover within the upper Palaeozoic basin. The results imply that the thickness of this conductive layer is considerably less than 100 m.

SUMMARY

The Ae forest MT survey has been described and details of its purpose and field operation have been provided. The performance of the new MT instrumentation will be described elsewhere. Data quality, particularly at low frequencies, was variable. This was an inevitable consequence of the learning curve associated with the operation of new equipment in a rapid reconnaissance survey. A great deal of useful technical information was obtained.

The results presented here are intended as an initial appraisal of the geoelectric structure encountered. The results are not final and are intended as a rapid 'turn-around' of the field measurements.

The 8 site NW-SE profile provides information on the crustal resistivity section from depths of several hundred metres through to depths greater than 30 km. Of the 8 soundings obtained only one sounding (site 005) appears to suffer static distortion. The data from this site will require correction (normalisation) if they are to be modelled correctly.

As expected from the outcrop geology along the profile, the two sites (007 and 008) to the SE of the profile detect what amounts to a thin conductive layer associated with the upper Palaeozoic sandstones of the basin around Lochmaben. Although further data modelling is required it is unlikely that the thickness of this layer can be resolved by the data bandwidth.

In terms of overall sounding characteristics the soundings along the profile form 3 groups. The c-response data from all sites (Figure 4) display the different characteristics of the 3 groups. Sites 007 and 008 define the first group largely by virtue of the near-surface conductive effect. These soundings are also the most 1-D through the upper crustal section. Sites 002 to 006 form the second group of sites with similar data characteristics. A major transition, in terms of overall data character, takes place between sites 001 and 002.

All sites display a transition from approximate 1-D behaviour within the upper crustal section through to 2-D by mid to lower crustal depths. Basically sites 002 to 008 are underlain by a relatively conducting (initial estimate of 100 ohm.m or less) mid to lower crustal layer. This deep seated conductive formation is responsible for the regional geoelectric anisotropy and the stable geoelectric strike directions discussed below.

The major crustal dislocation in resistivity structure that takes place between site 001 and 002 (an along profile distance of 2.2 km) must require a 2-D interpretation. The approximate and 1-D

resistivity profiles (figure 8) in the vicinity of this feature are unlikely to be correct. In fact there is a clear indication of progression of tensor derived data characteristics (dimensional weights and azimuths) to the SE of site 002.

The most stable geoelectric strike azimuths occur at the lowest frequencies where the 2-D regional influence is at a maximum. The azimuths obtained show a degree of progression along the profile. At site 002 the regional low frequency azimuth is +45 degrees and is found to rotate to +50 to +60 degrees by sites 003 and 004. At sites 006, 007 and 008 the regional strike direction is between +60 and +70 degrees. A more complete assessment of azimuths will be undertaken when the vertical field data have been assessed.

The results acquired obviously deserve more thorough 1-D and 2-D modelling to generate an appropriate cross-section of resistivity structure. Although such model refinement will be undertaken, the procedure will be difficult due to (i) the variable quality of the low frequency data, (ii) it will be necessary to model a crustal scale section using a profile length of only 14 km and (iii) the main lateral change in resistivity occurs in the vicinity of the 2 northern-most soundings. As the most immediate outcome of the survey we note a possible correlation of the resistivity transition with the NW-SE geochemical trend discussed by Stone et al. (1991, Fig. 5, line Z).

REFERENCES.

Banks, R.J., Beamish, D. and Geake, M.J., 1983. Magnetic variation anomalies in northern England and southern Scotland. *Nature*, 303, 516-518.

Beamish, D., 1986. Geoelectric structural dimensions from magnetotelluric data : methods of estimation, old and new. *Geophysics*, 51, 1298-1309.

Dobrin, M.B. and Savit, C.H., 1988. *Introduction to Geophysical Prospecting* (Fourth Edition). McGraw-Hill Publishers.

Kimbell, G.S., 1991. Magnetic anomalies and the deep structure of the Iapetus convergence zone, *Geophys. J. Int.*, 104, 687 (Abstract).

Stone, P., Floyd, J.D., Barnes, R.P. and Lintern, B.C., 1987. A sequential back-arc and foreland basin thrust duplex model for the Southern Uplands of Scotland, *Journal of the Geological Society, London*, 144, 753-764.

Stone, P., Green, P.M., Lintern, B.C., Plant, J.A., Simpson, P.R. and Breward, N., 1991. Geochemistry characterizes provenance in southern Scotland, *Geology Today*, Sep.-Oct., 177-181.

FIGURE CAPTIONS.

Figure 1. Location of MT survey profile (+ to +) on geological map of the Southern Uplands after Stone *et al* (1987).

Figure 2. Location of MT survey profile (+ to +) on geomagnetic variation anomaly map of the Southern Uplands. Map data from Banks *et al* (1983).

Figure 3. Detailed site locations of the MT survey. Sites are referred to as 001 to 008 in the text.

Figure 4. Sounding data in the XY and YX measured tensor components at the 8 sites. The XY component is the principal sounding looking north and the YX component is the principal sounding looking east. Error bars are +/- one standard error.

Figure 5. Sounding data at all 8 sites. The average (or effective) invariant has been used to determine the complex c-response, plotted in its real and imaginary components. The real part of the c-response gives a measure of the effective penetration as a function of frequency. Site 001 data are open circles, solid stars are data from sites 002-006 and solid circles are data from sites 007 and 008.

Figure 6. Dimensional weights at the 8 sites. The weights give an indication of the relative geoelectric structural influences on the sounding data. D1 is the one-dimensional indicator (open circles). D2 is the two-dimensional indicator (solid circles) and D3 is the three-dimensional indicator (open crosses).

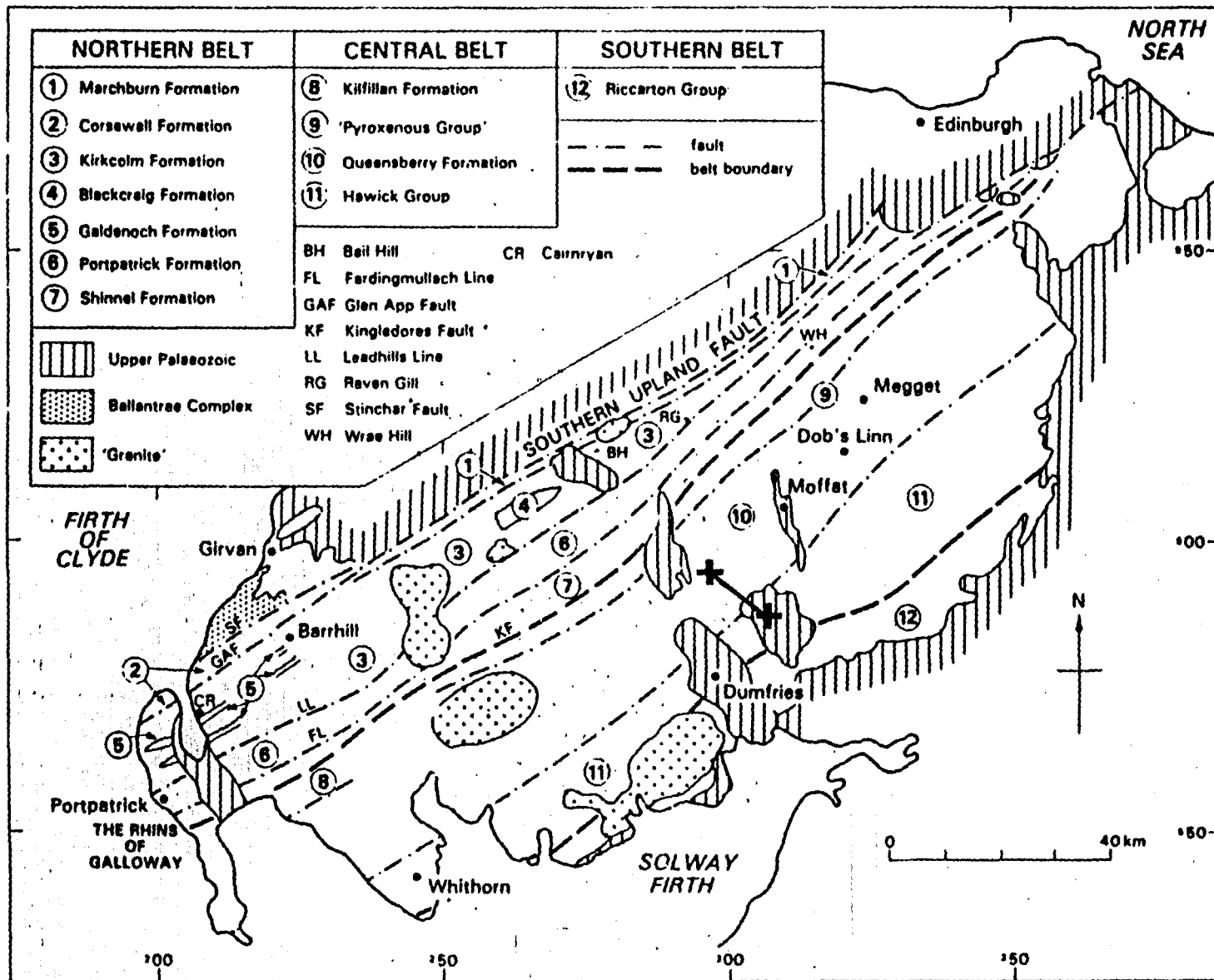
Figure 7. Geoelectric strike (2-D) directions at the 8 sites. The azimuths have been obtained by conventional tensor rotation. Azimuths refer to grid north (positive clockwise) and standard errors are shown.

Figure 8. Approximate 1-D inversions (Bostick-Niblett transform) at the 8 sites. The average (or effective) sounding curves have been used. The left diagrams give the result in log(depth) scale while the right diagrams give the same data in linear depth scale.

TABLE 1. AE FOREST MT SURVEY. SITE DETAILS.

The 8 sites comprising the Ae forest survey are listed 001-008. The profile consists of a NW-SE traverse with site 001 defining the northern-most site and site 008 defining the southern-most site. The FIELD-ID is a field (data file) code which also refers to the chronological order of the survey (i.e. 111 to 888). Date refers to site occupation. National Grid coordinates and elevations (from 1:10000 O.S. maps) are given in metres.

SITE CODE	FIELD ID	DATE	EASTING (m)	NORTHING (m)	HEIGHT (m)
001	444	13-09-91	296590	596420	220
002	333	12-09-91	298590	595355	280
003	222	11-09-91	299730	594000	290
004	555	14-09-91	299820	592740	340
005	111	10-09-91	300920	592140	249
006	666	15-09-91	302340	591000	297
007	777	16-09-91	303770	588690	82
008	888	17-09-91	306100	587050	58



Geological map of the Southern Uplands showing lithostratigraphic divisions, major faults, boundaries between the belts and localities mentioned in the text.

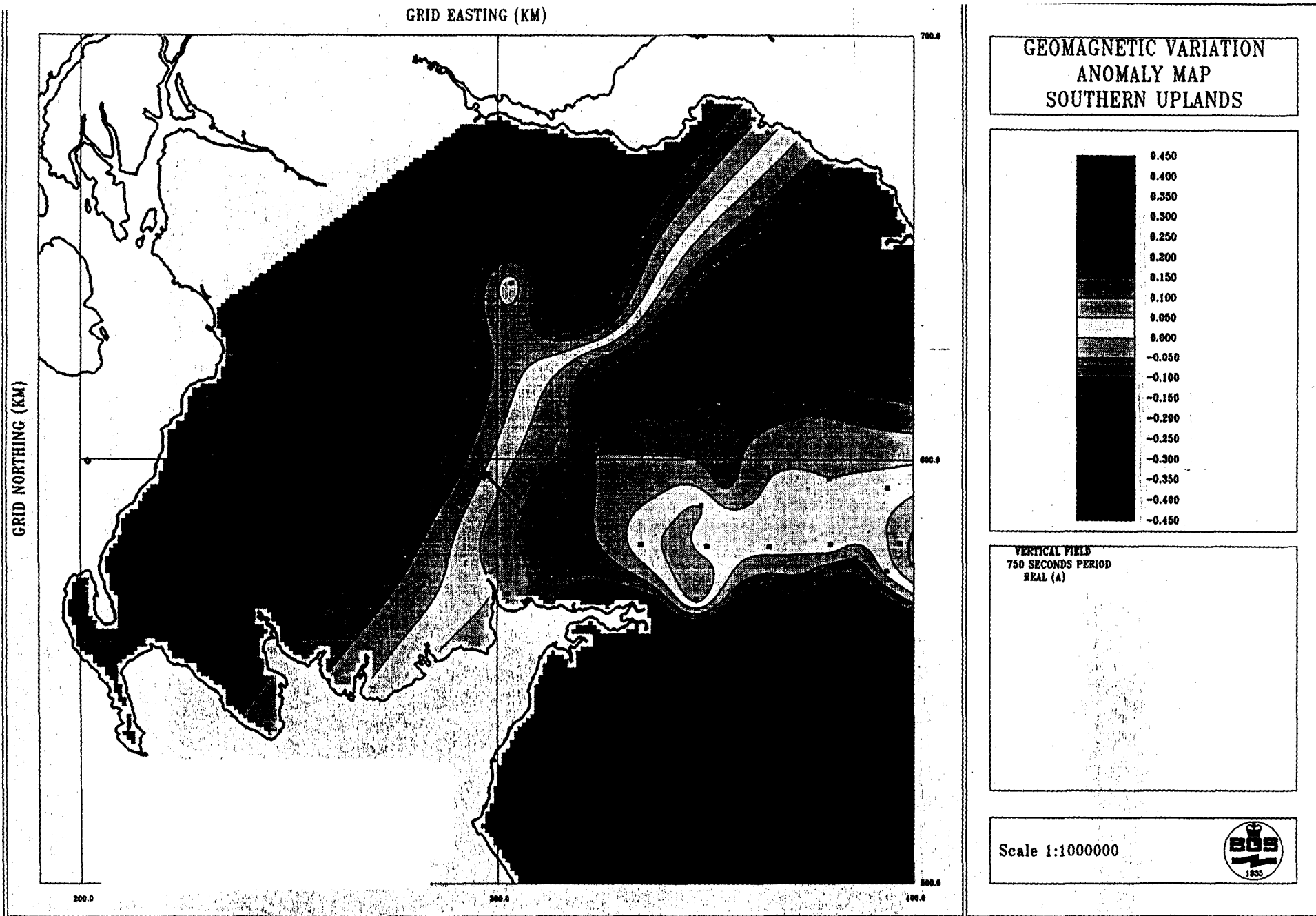


Fig. 2

MT SURVEY -- SOUTHERN UPLANDS
AE FOREST --- SITE LOCATIONS

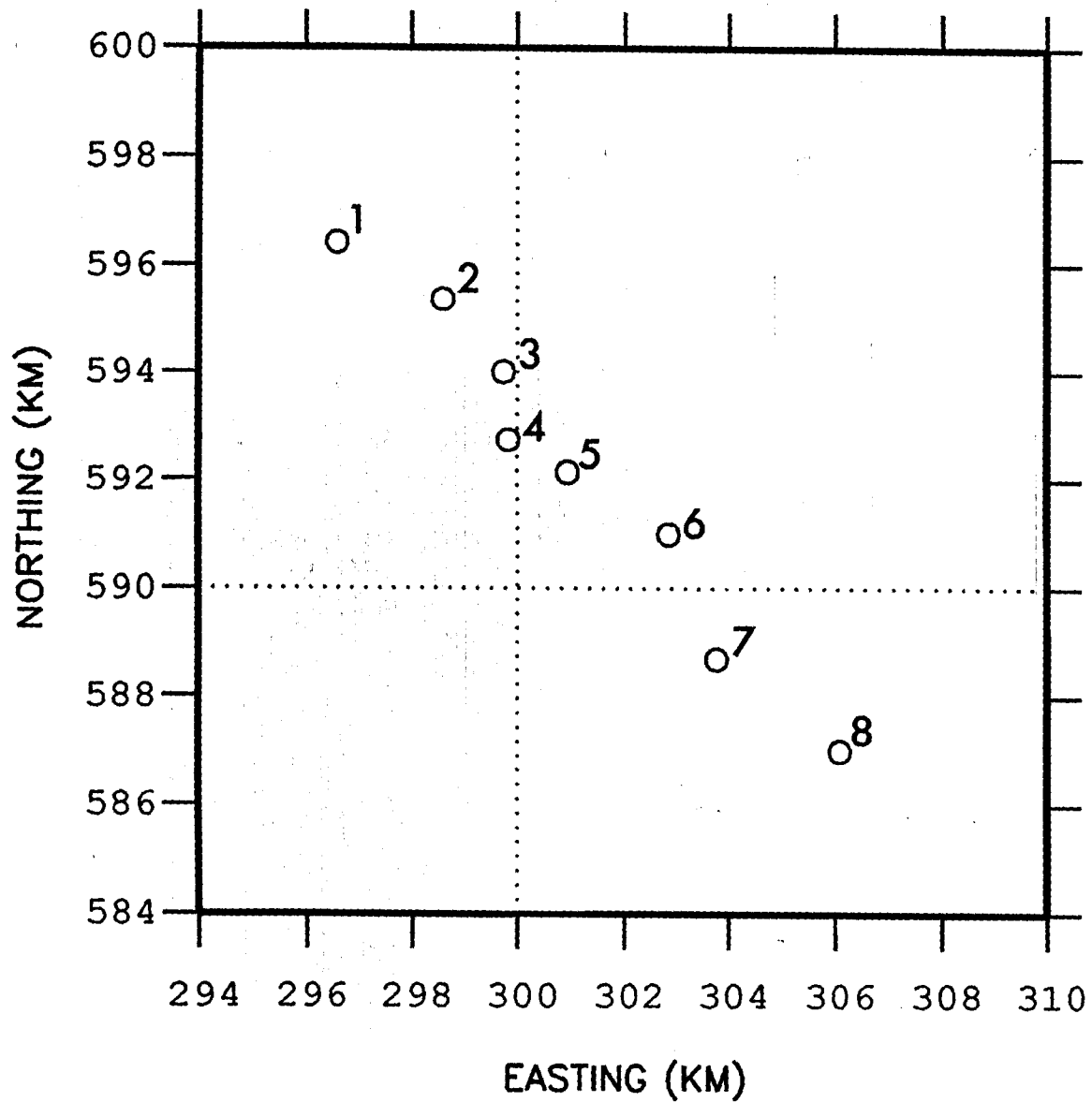
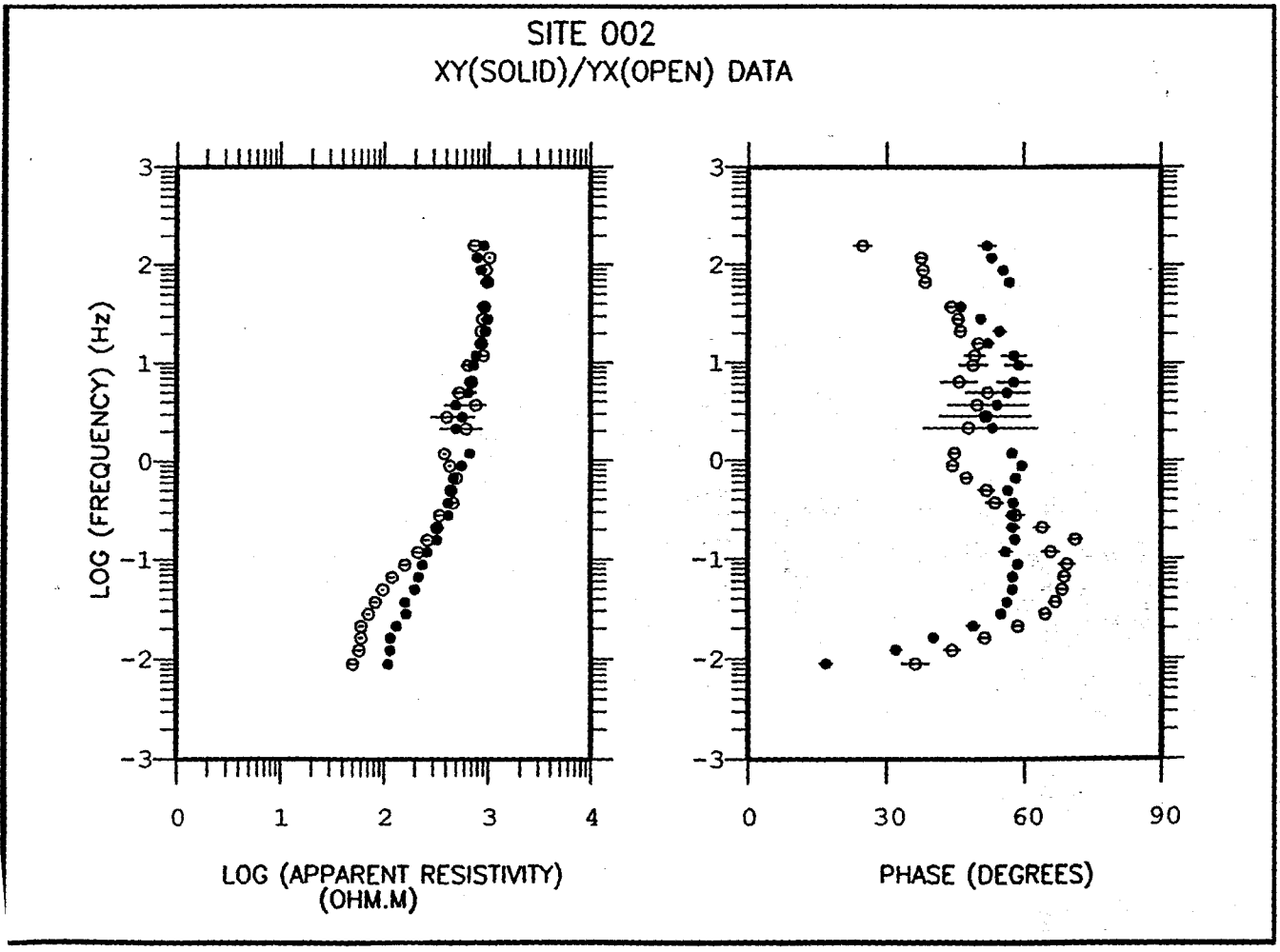
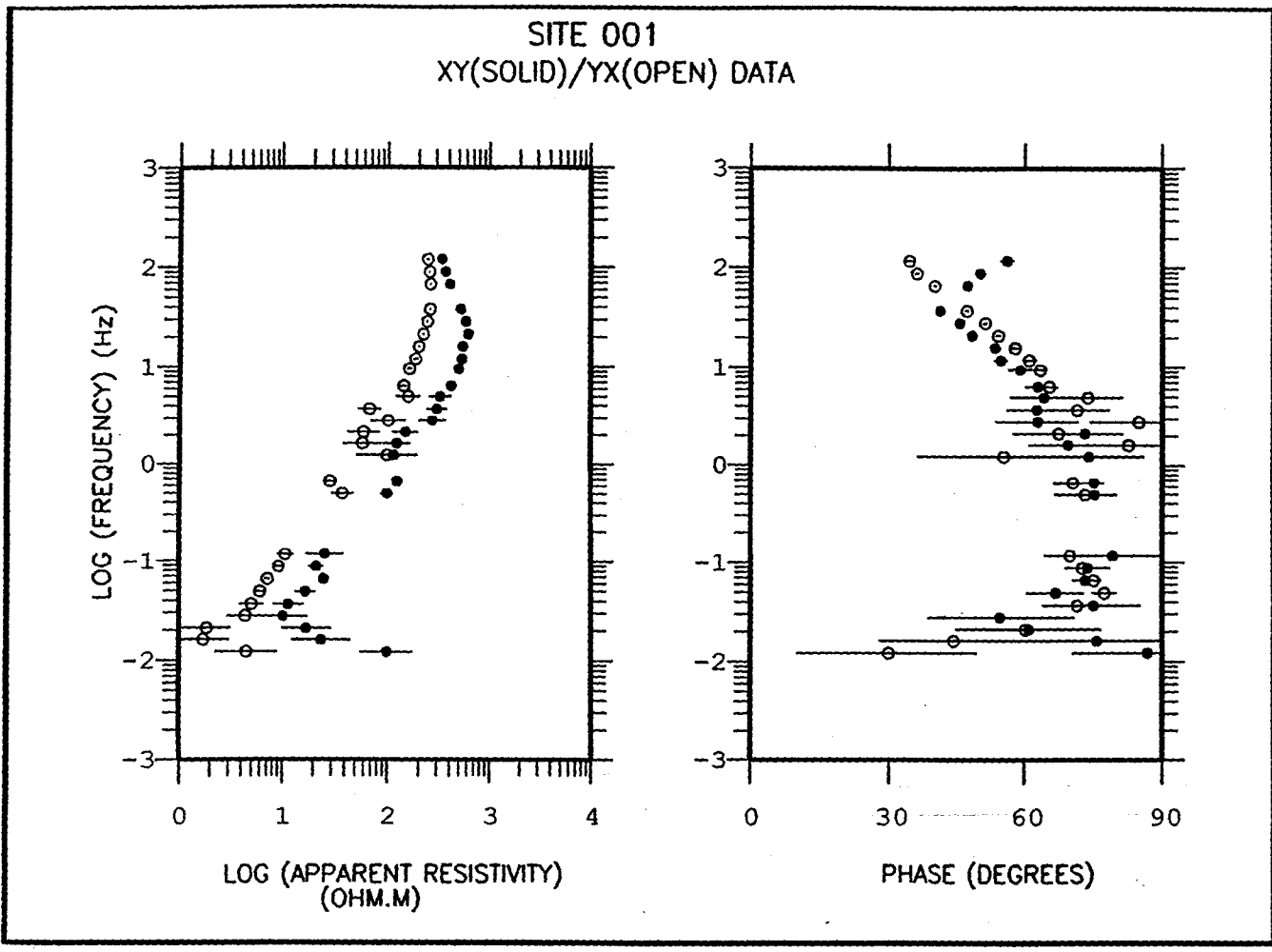
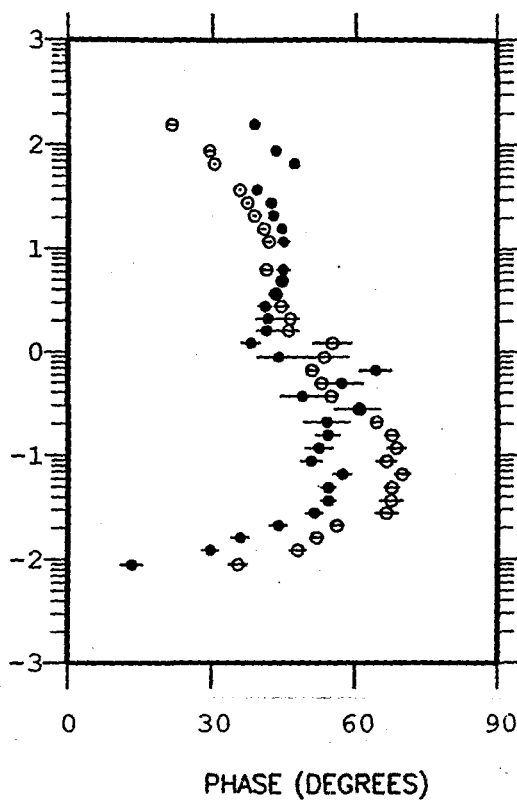
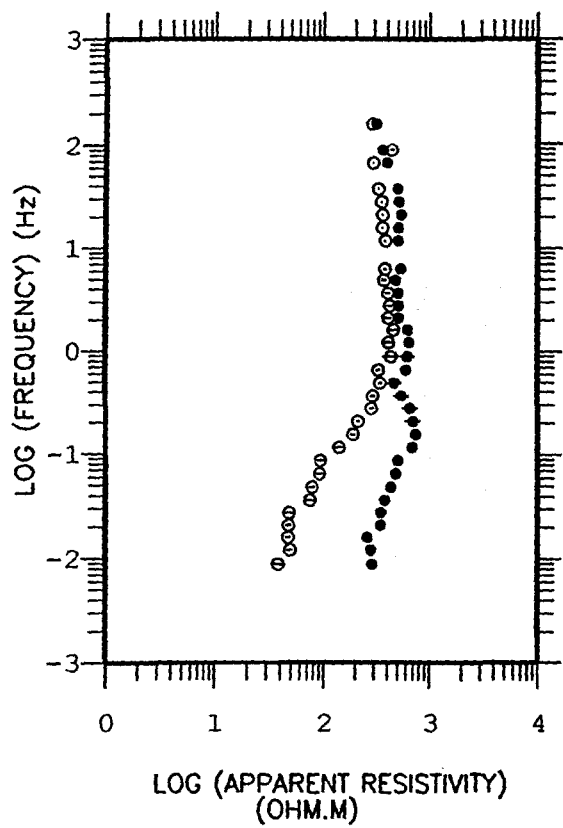


Fig.

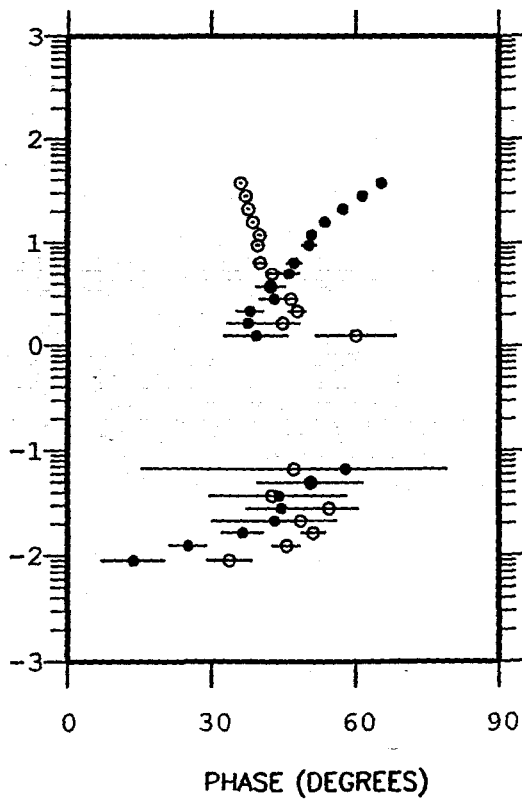
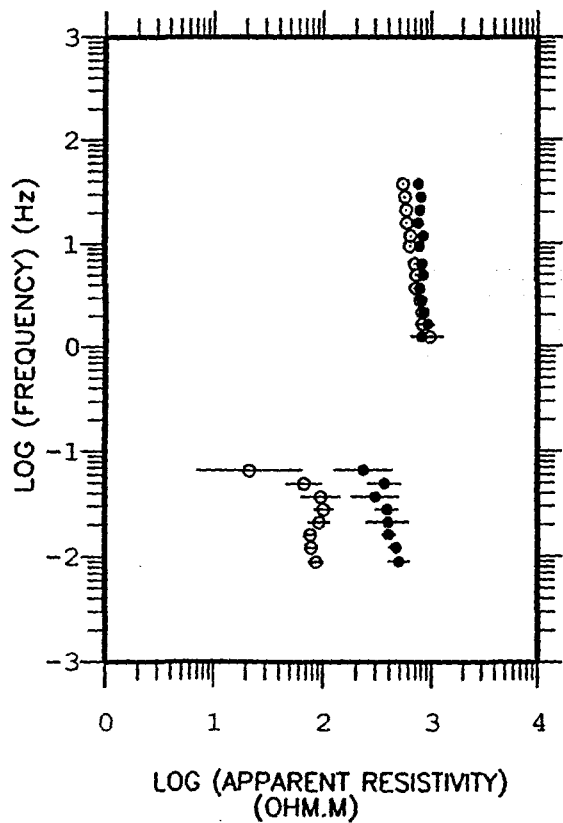
Fig.



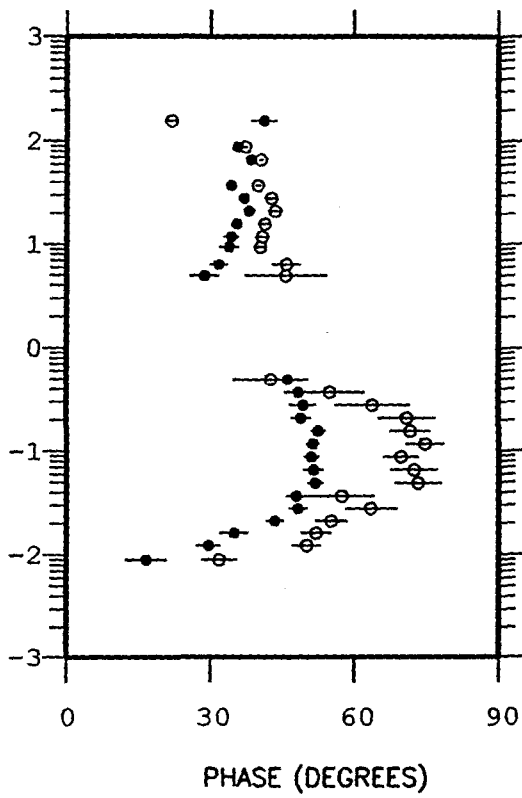
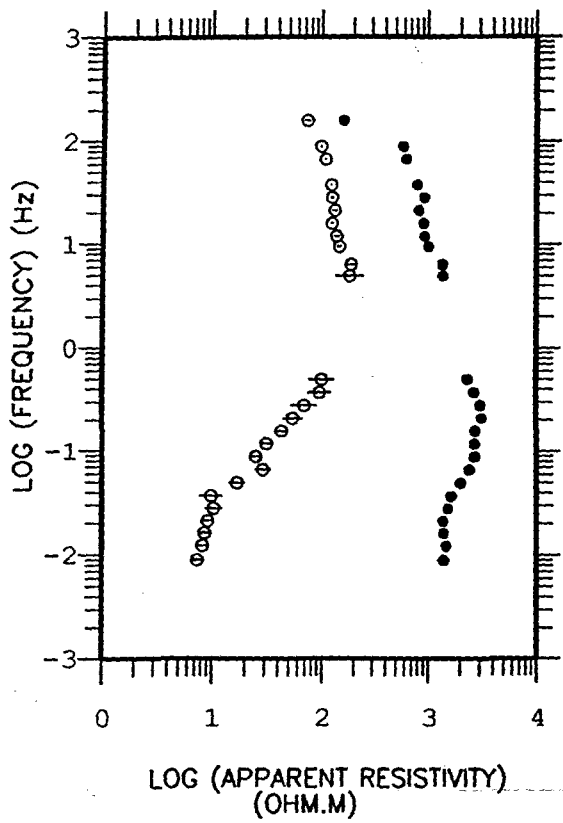
SITE 003
XY(SOLID)/YX(OPEN) DATA



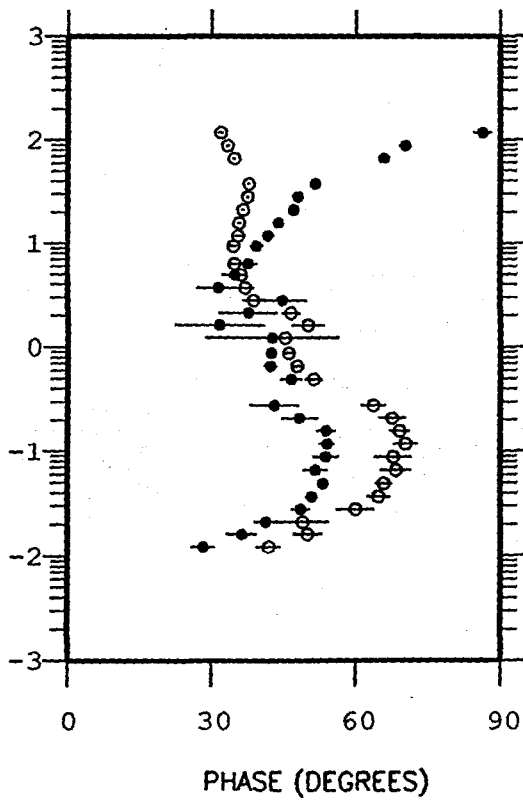
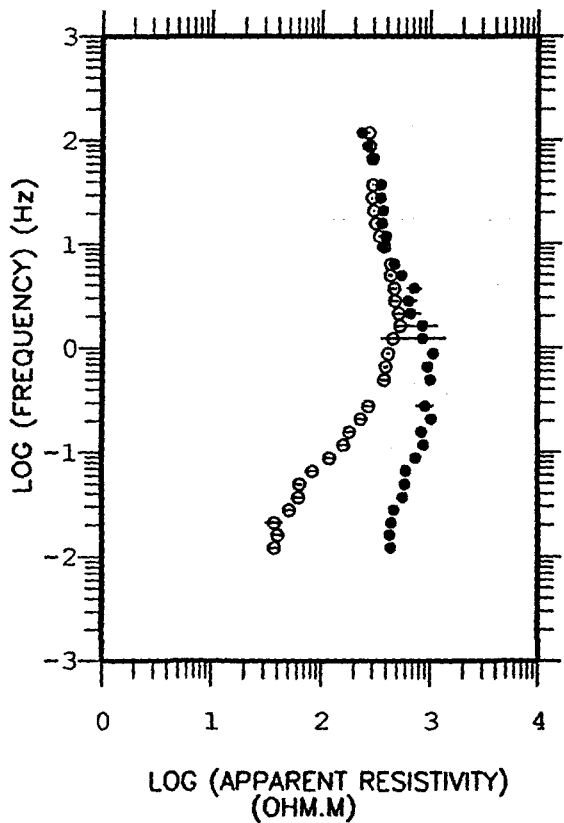
SITE 004
XY(SOLID)/YX(OPEN) DATA



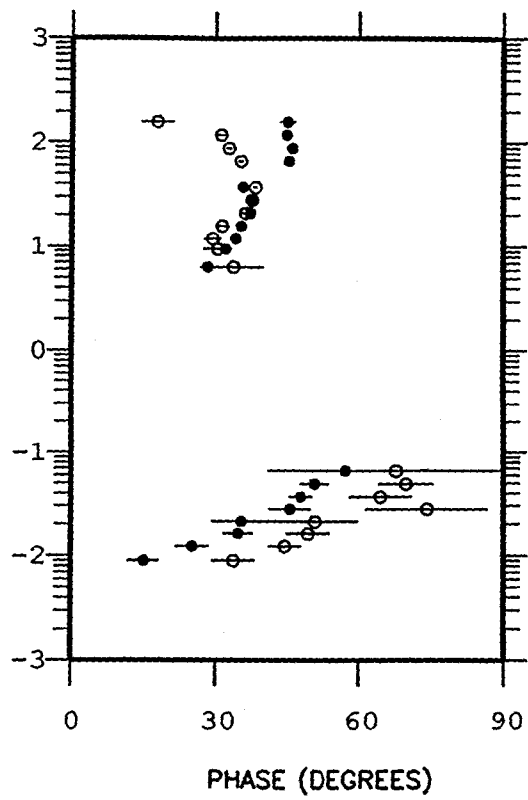
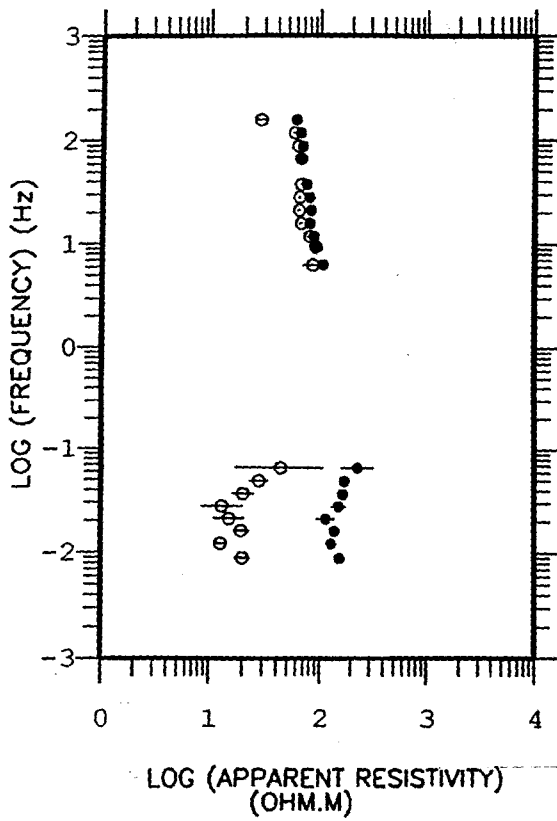
SITE 005
XY(SOLID)/YX(OPEN) DATA



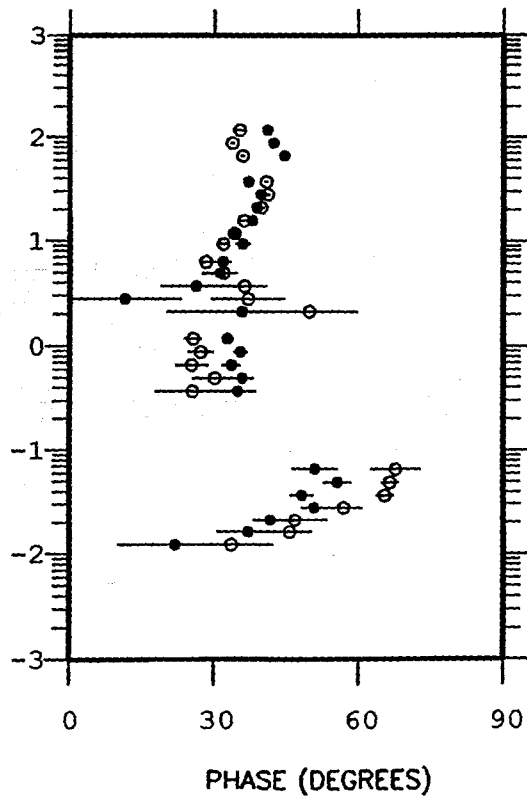
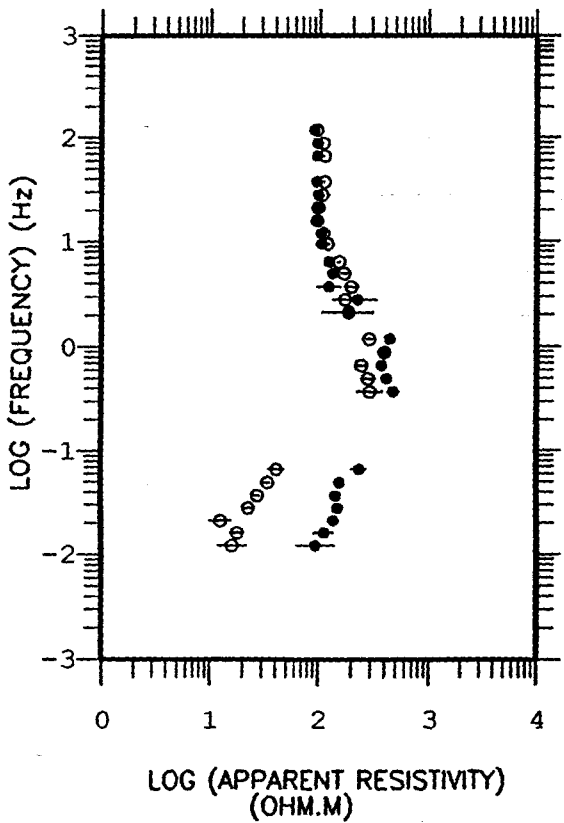
SITE 006
XY(SOLID)/YX(OPEN) DATA



SITE 007
XY(SOLID)/YX(OPEN) DATA



SITE 008
XY(SOLID)/YX(OPEN) DATA



ALL SITES -RAV-
EFFECTIVE PENETRATIONS (ReC)

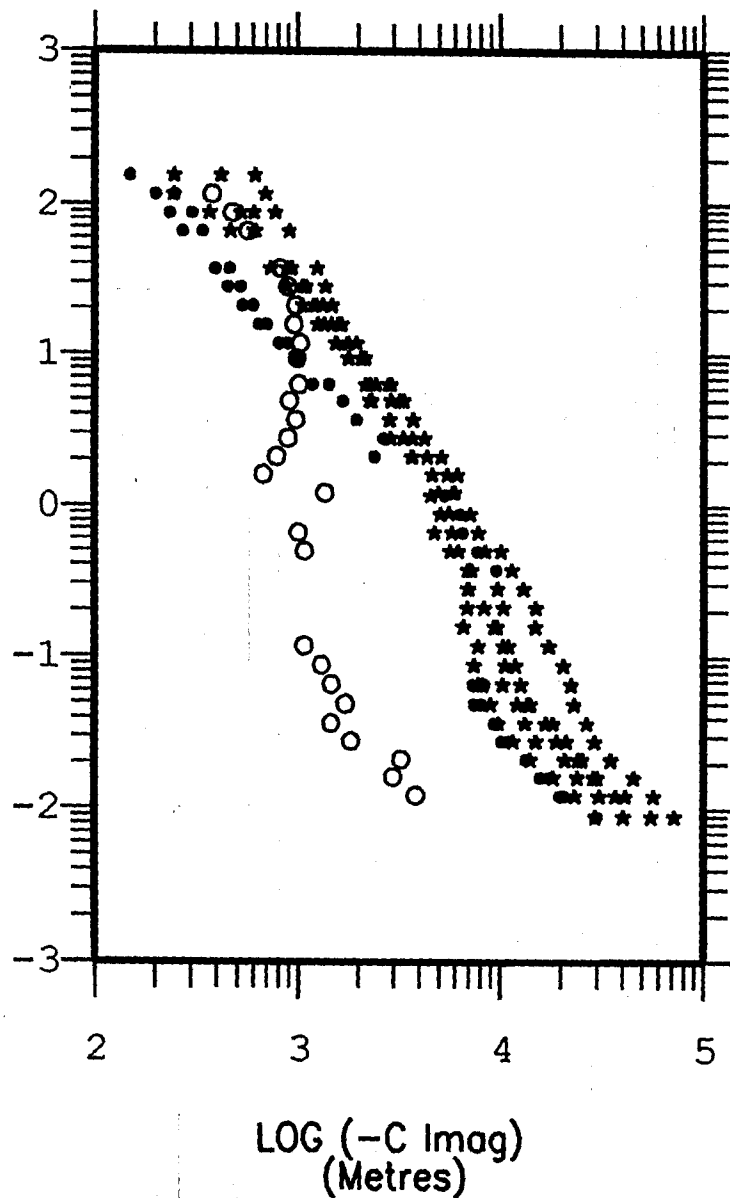
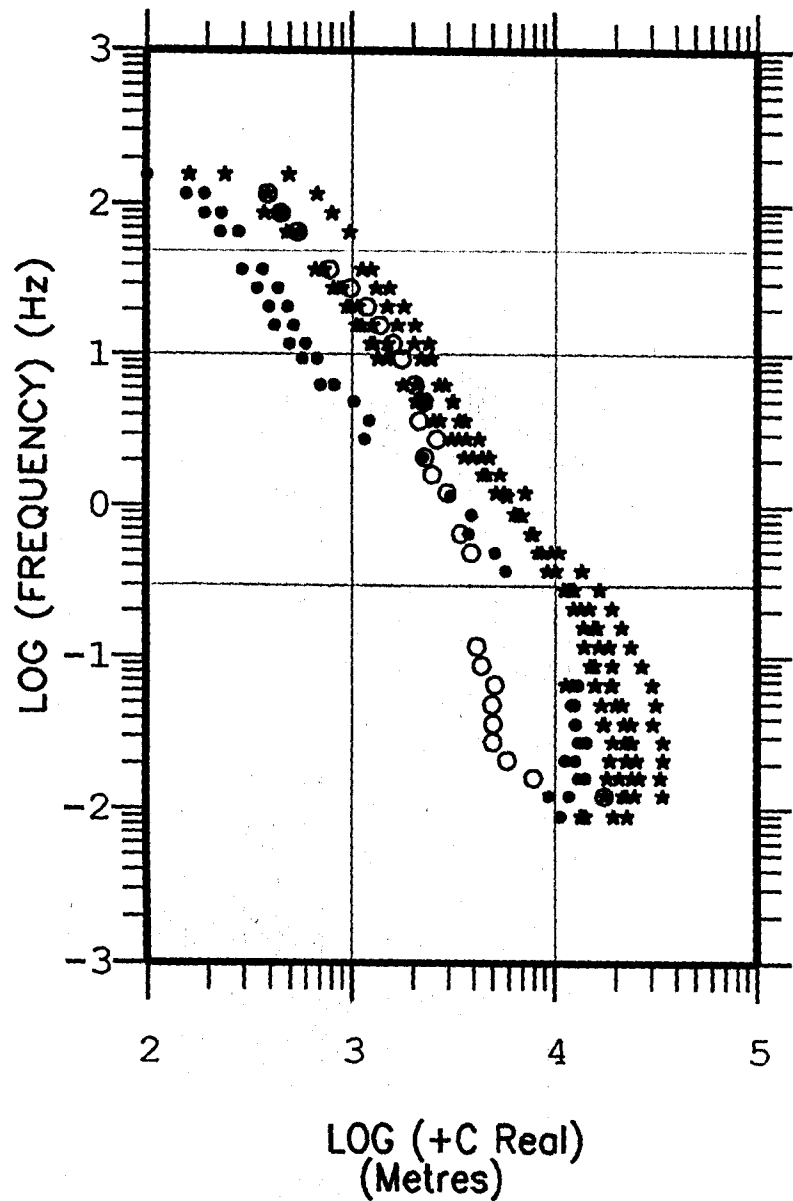
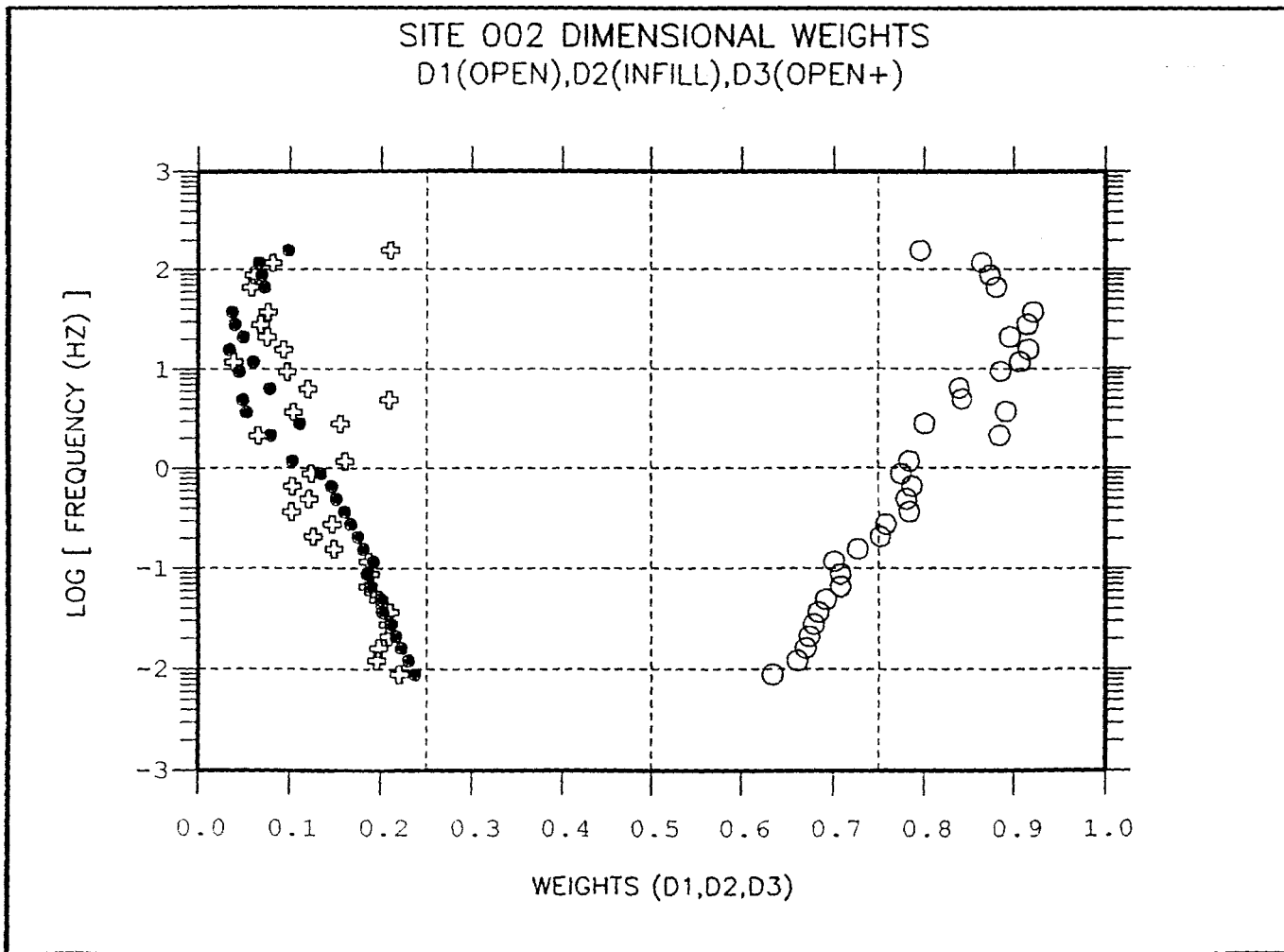
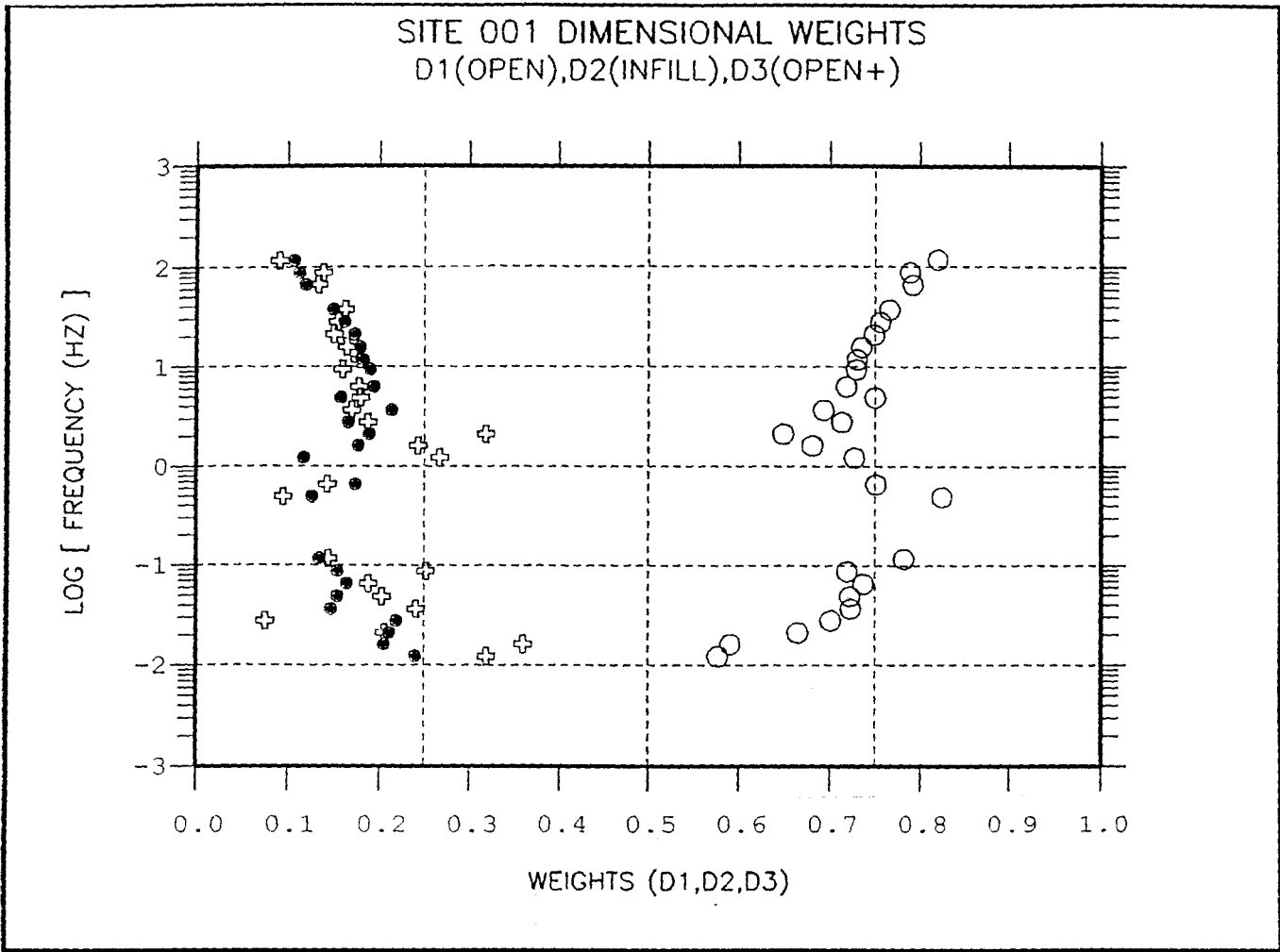
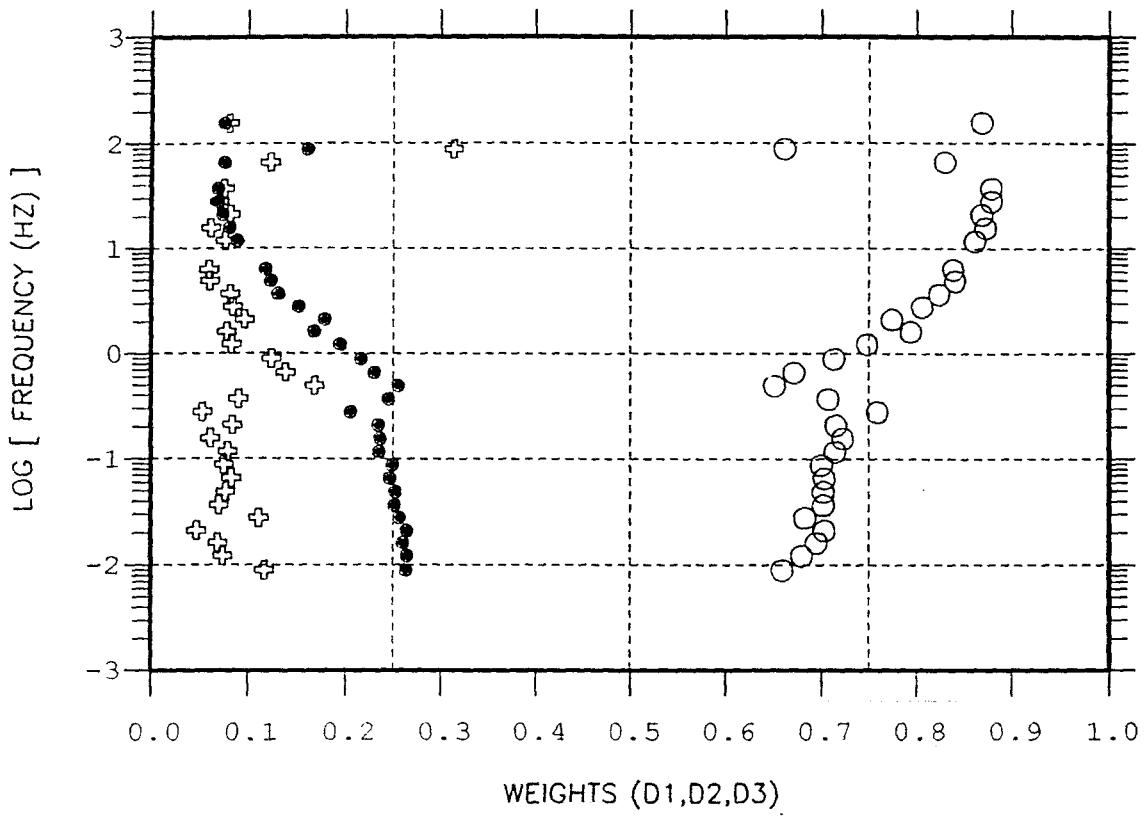


Fig.5

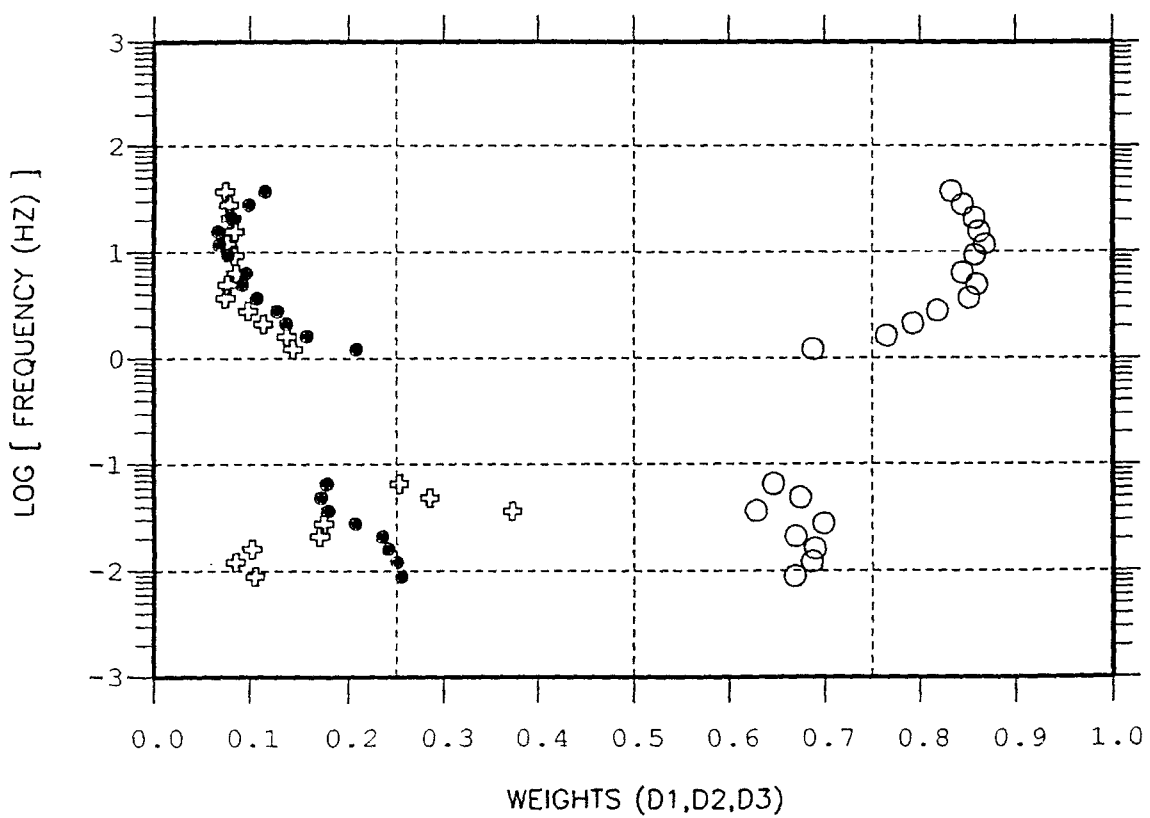
Fig.t



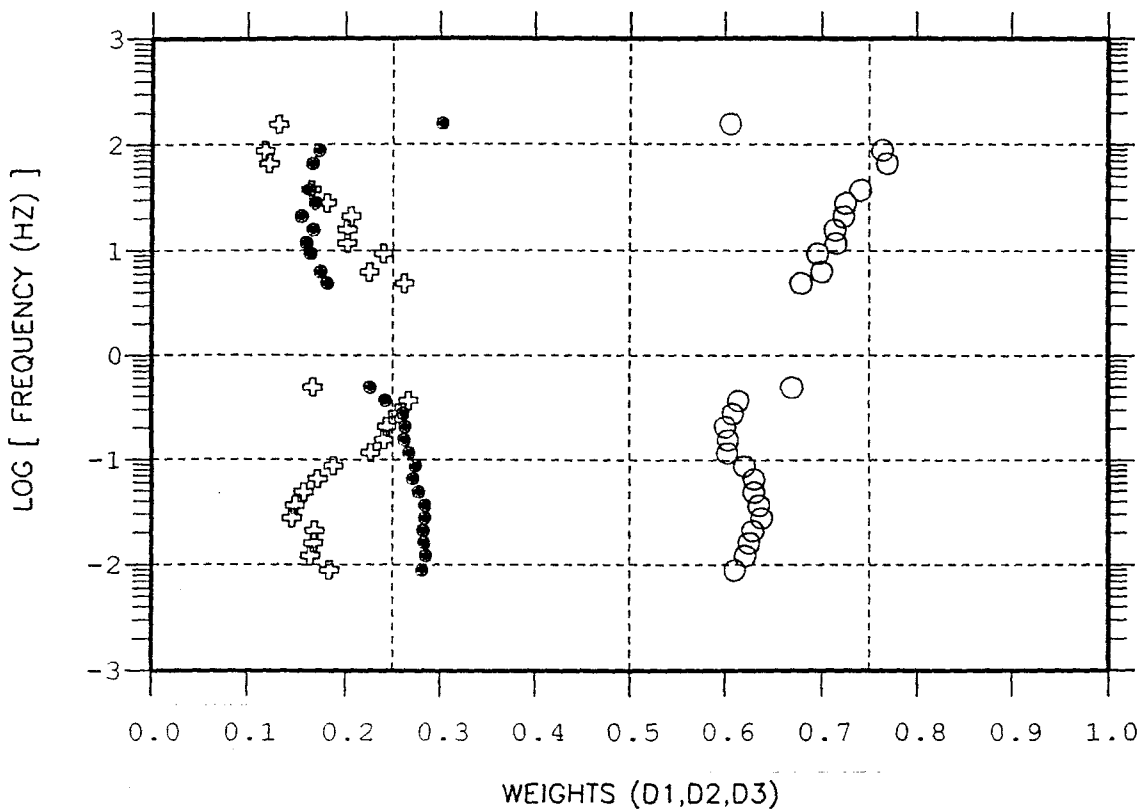
SITE 003 DIMENSIONAL WEIGHTS
D1(OPEN),D2(INFILL),D3(OPEN+)



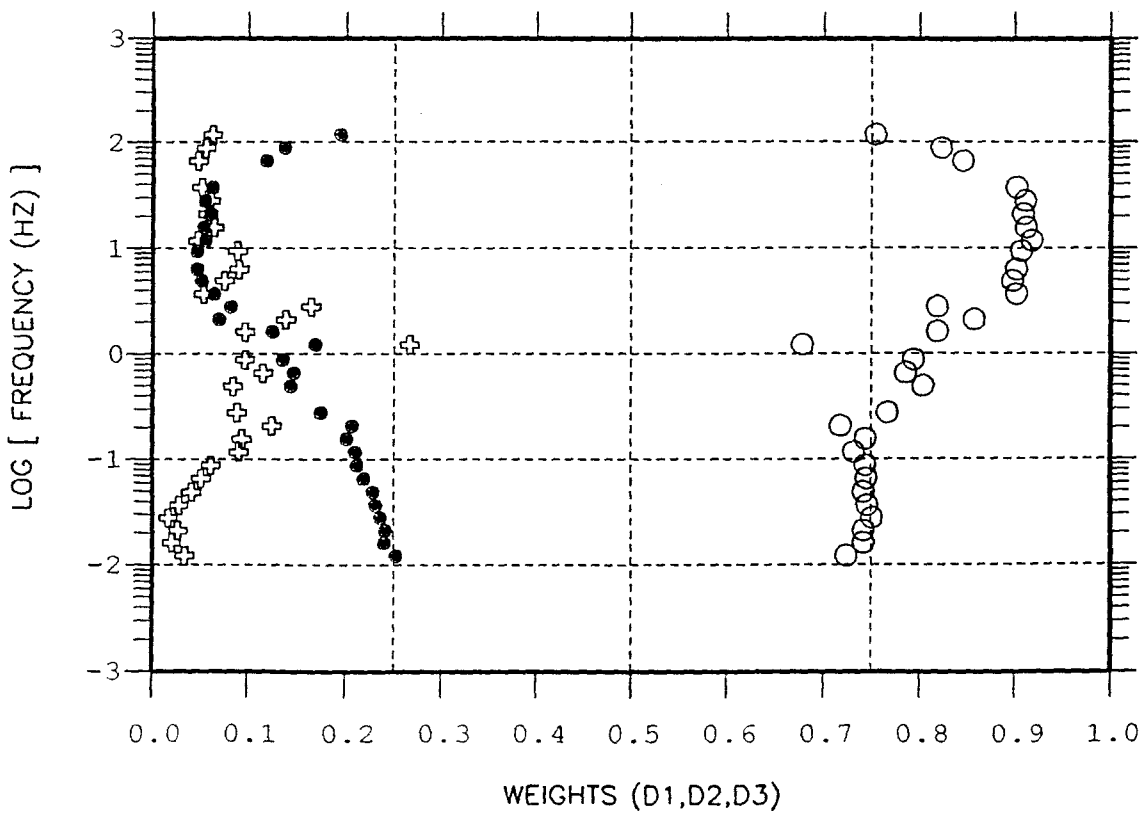
SITE 004 DIMENSIONAL WEIGHTS
D1(OPEN),D2(INFILL),D3(OPEN+)



SITE 005 DIMENSIONAL WEIGHTS
D1(OPEN),D2(INFILL),D3(OPEN+)



SITE 006 DIMENSIONAL WEIGHTS
D1(OPEN),D2(INFILL),D3(OPEN+)



SITE 007 DIMENSIONAL WEIGHTS
D1(OPEN),D2(INFILL),D3(OPEN+)

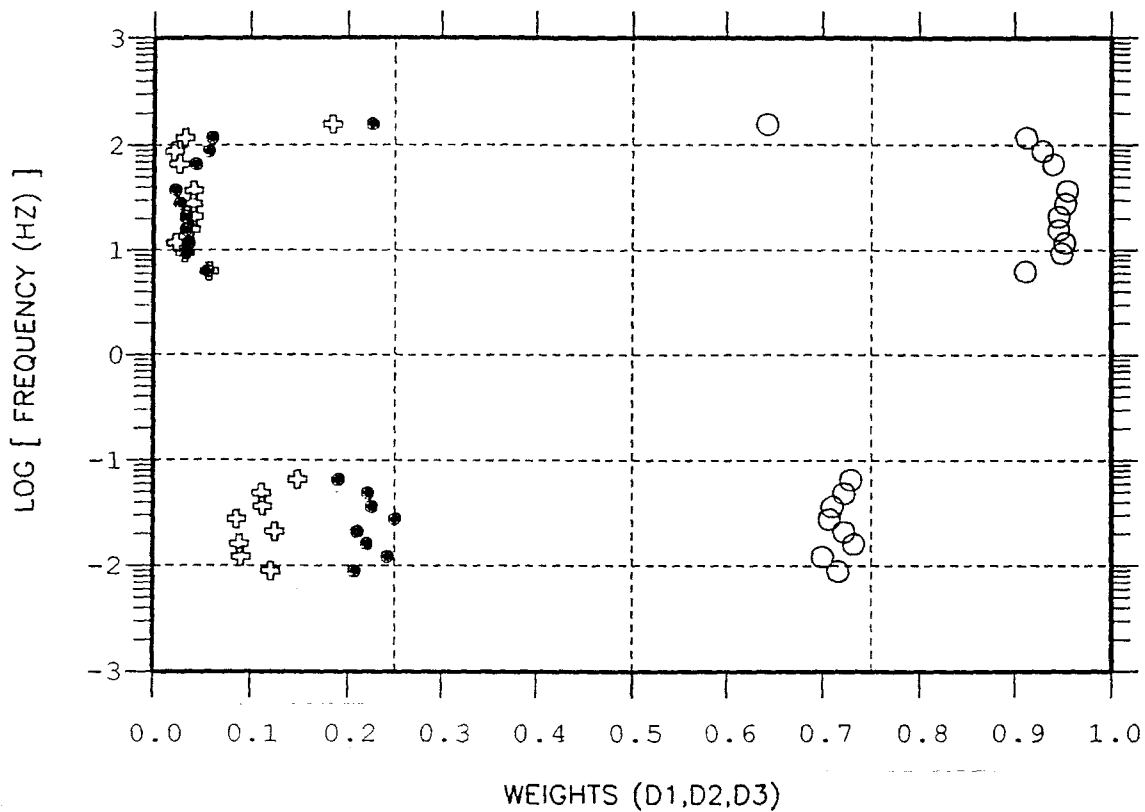
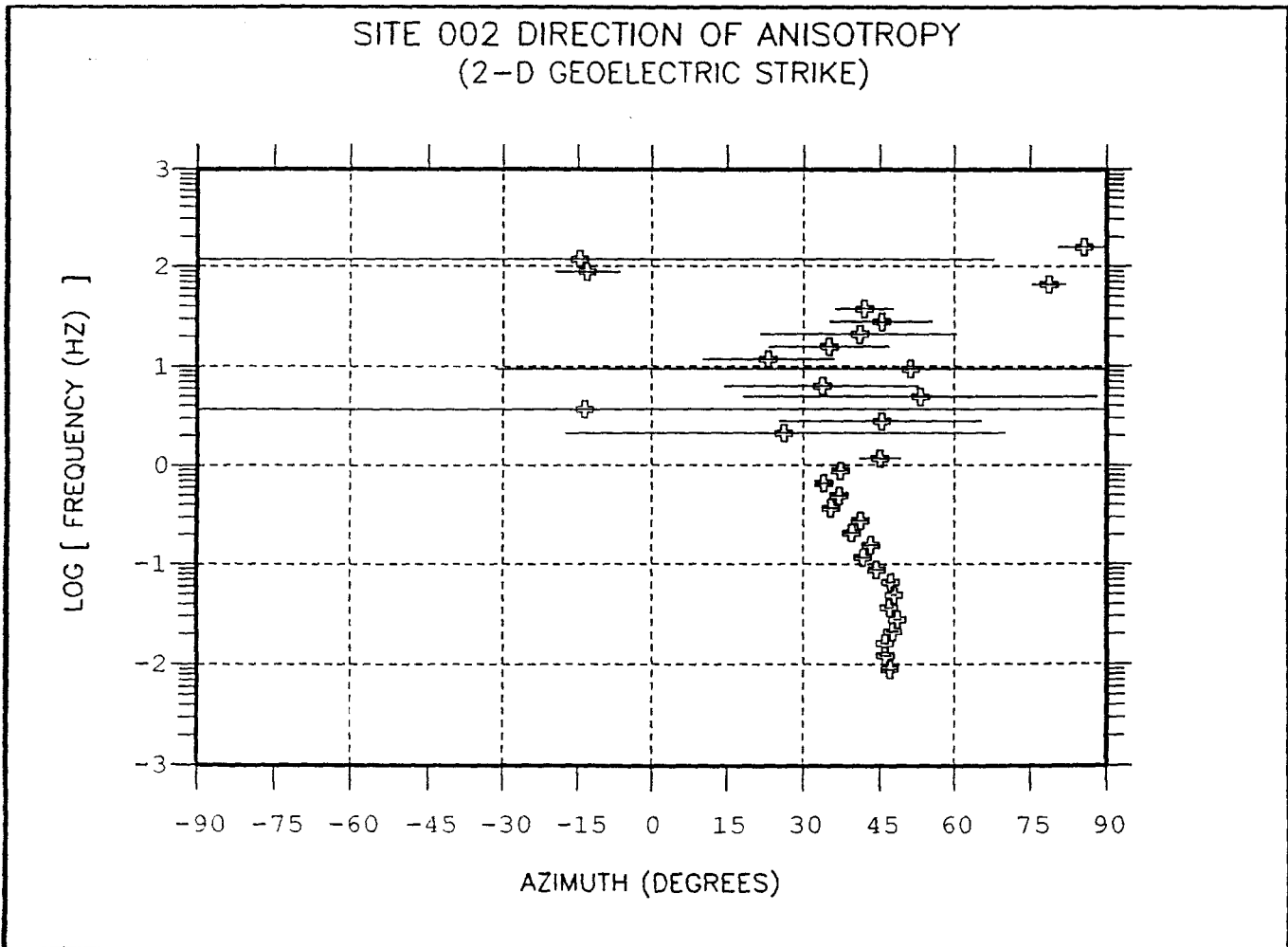
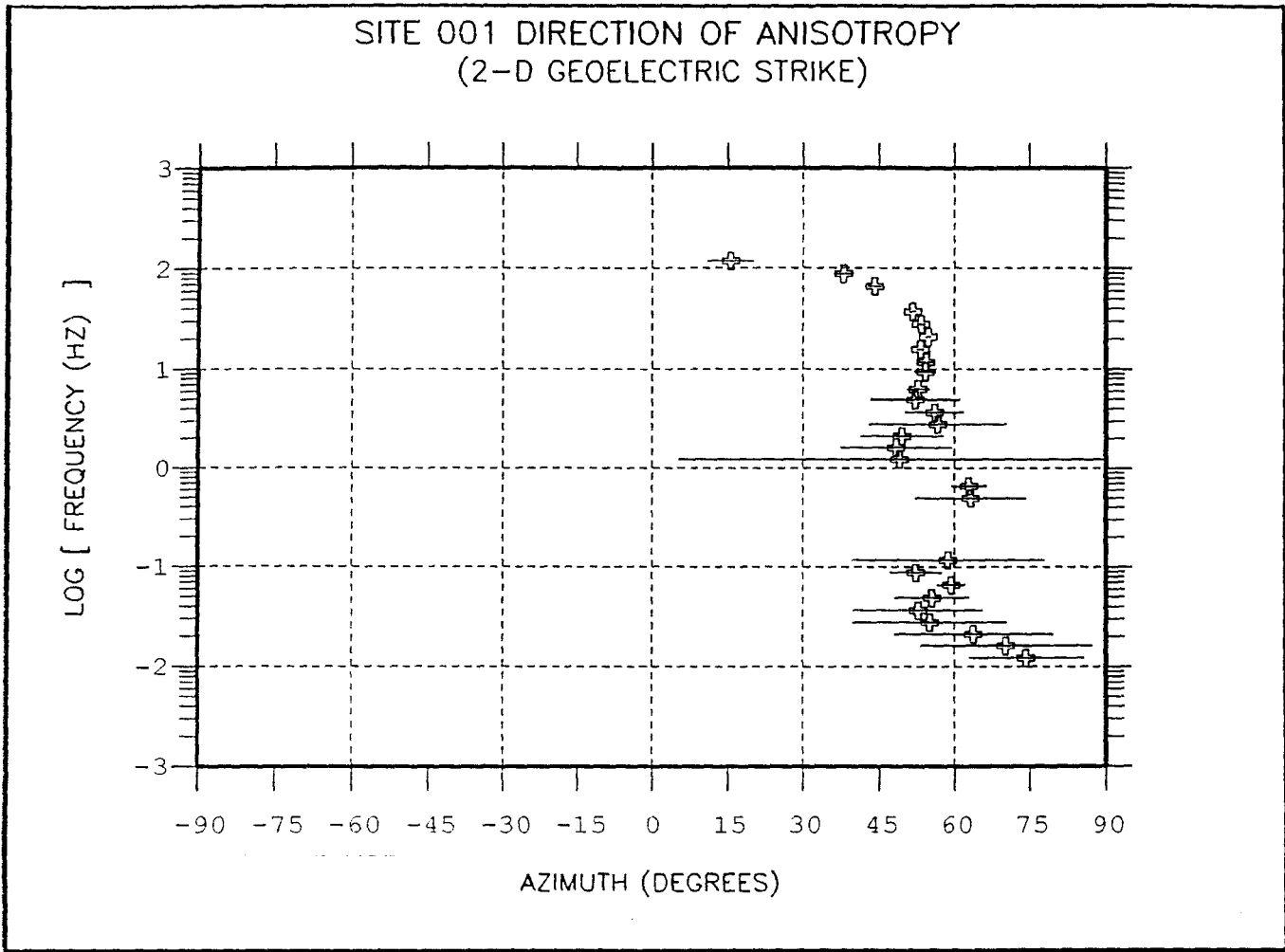
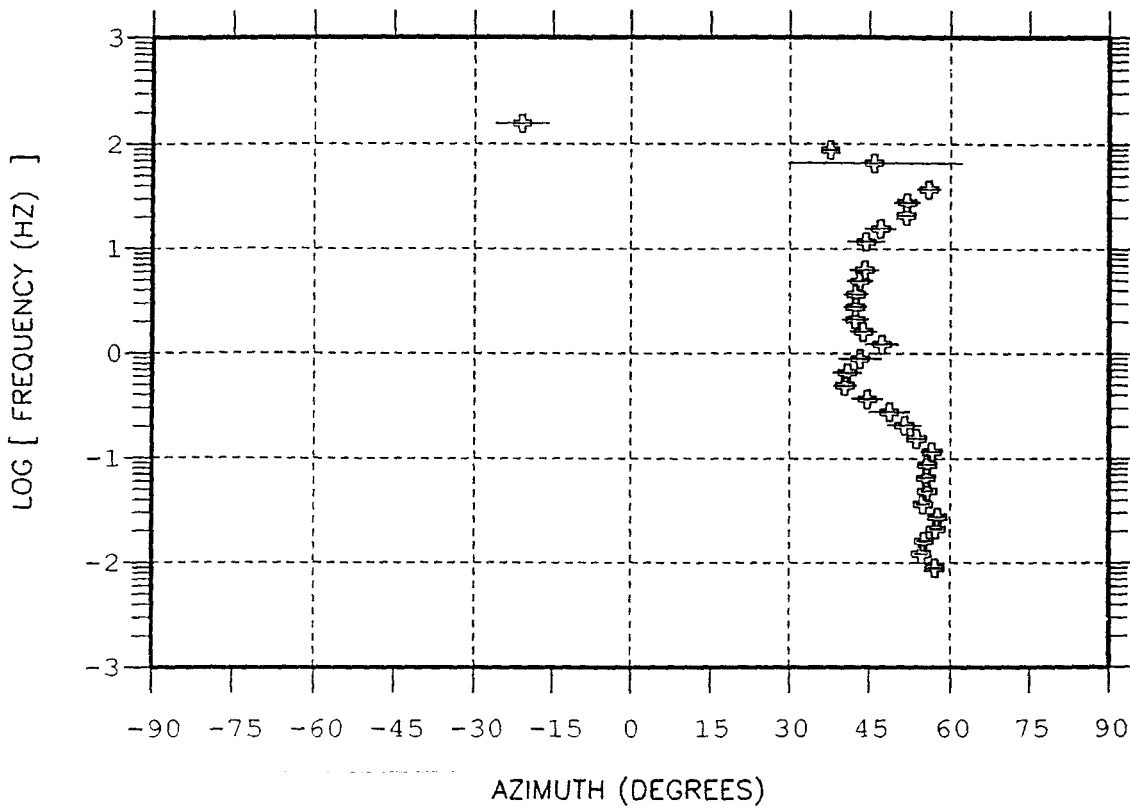


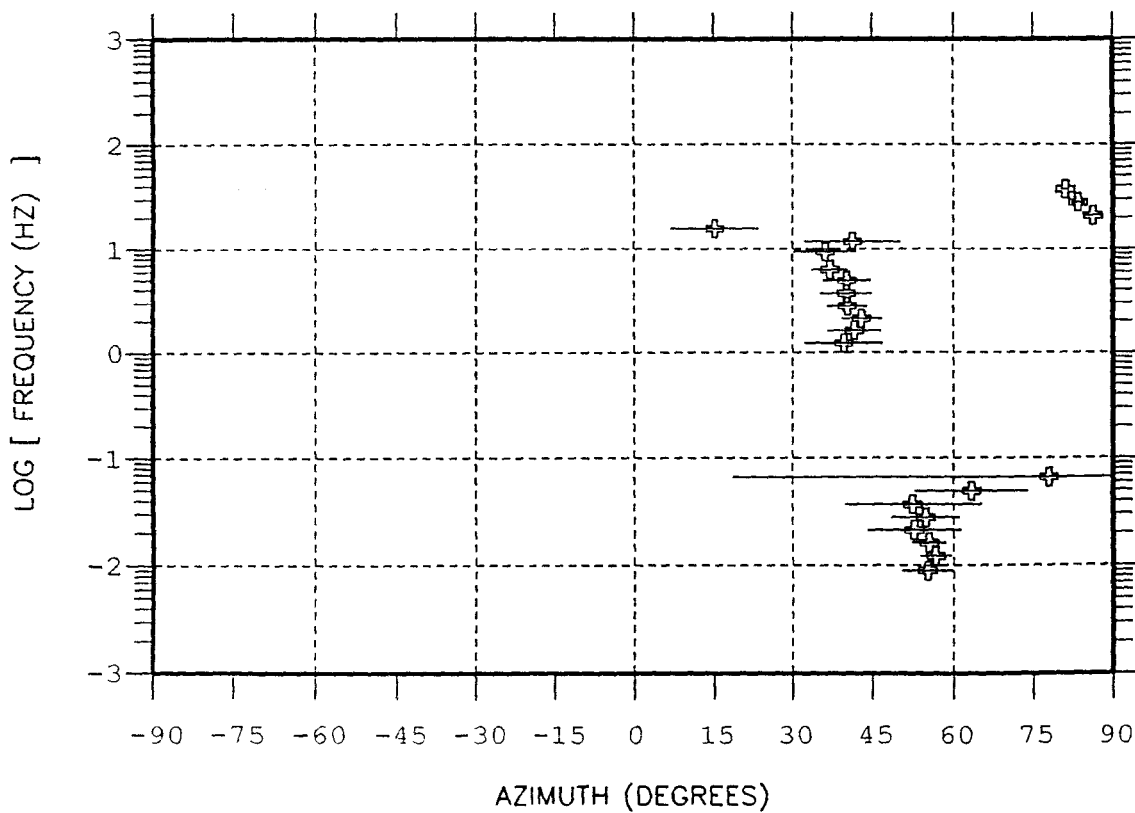
Fig. 7



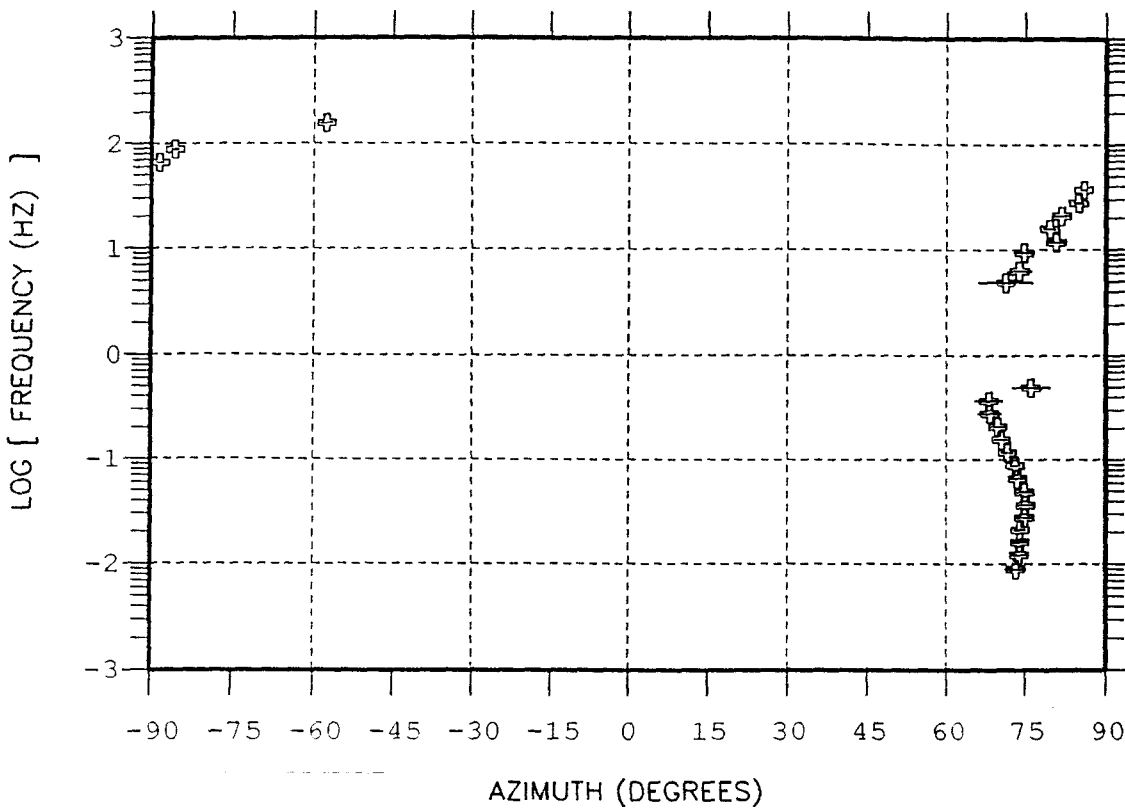
SITE 003 DIRECTION OF ANISOTROPY
(2-D GEOELECTRIC STRIKE)



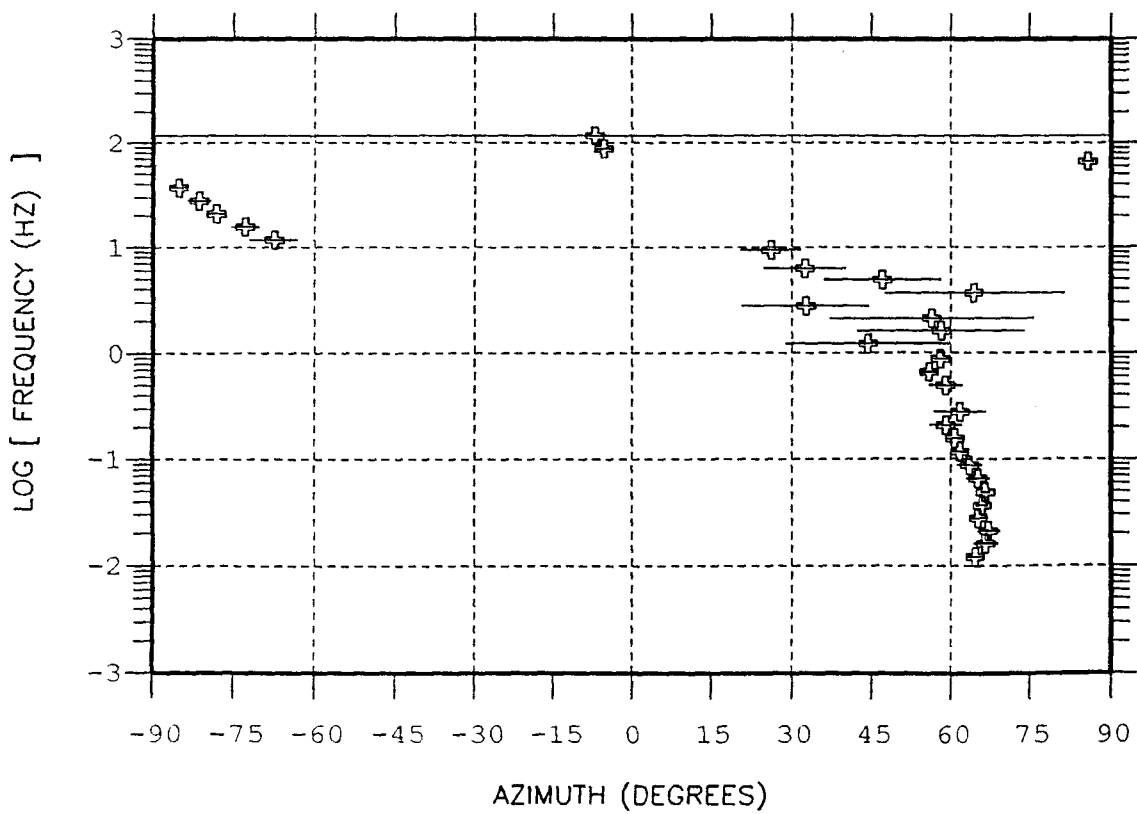
SITE 004 DIRECTION OF ANISOTROPY
(2-D GEOELECTRIC STRIKE)



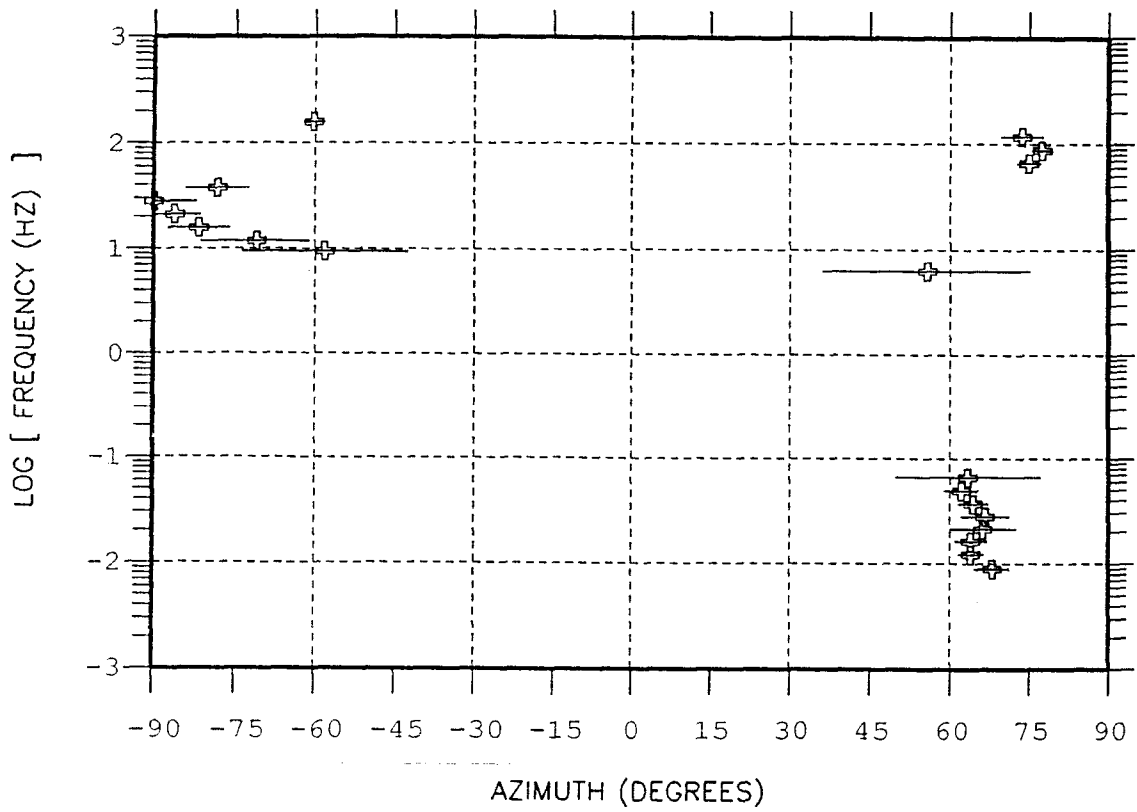
SITE 005 DIRECTION OF ANISOTROPY
(2-D GEOELECTRIC STRIKE)



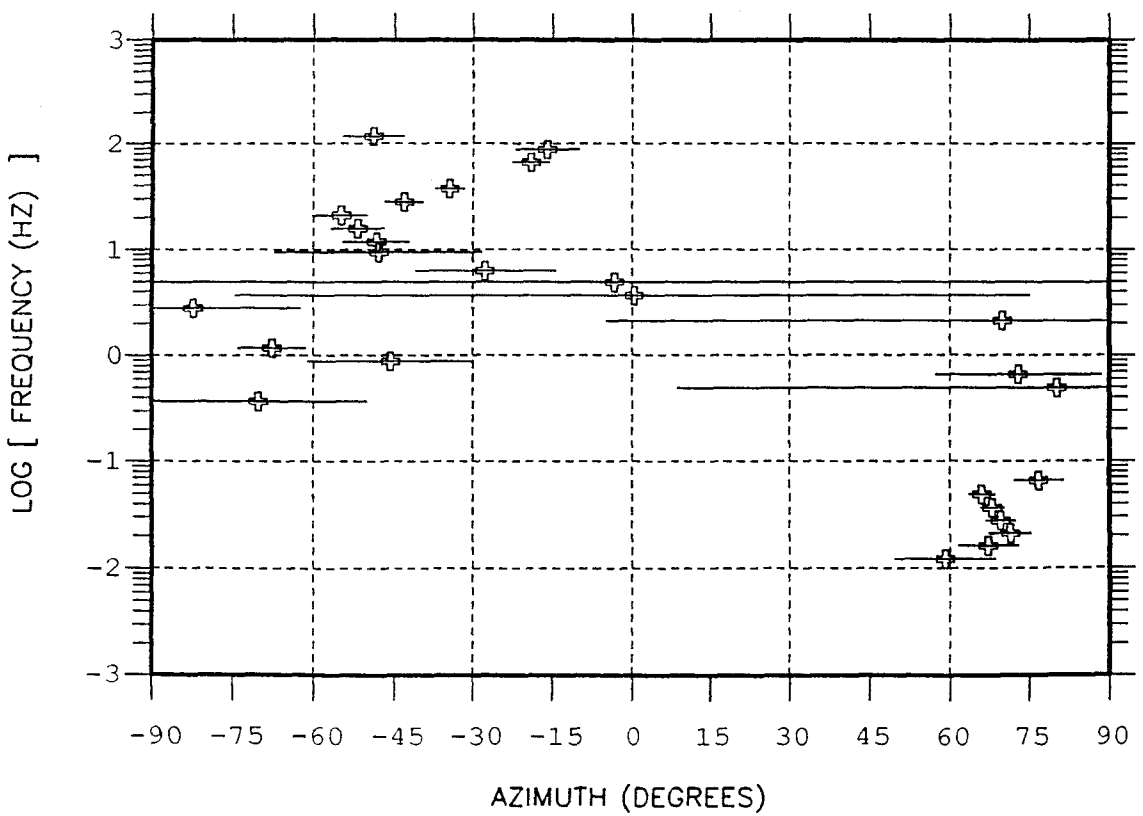
SITE 006 DIRECTION OF ANISOTROPY
(2-D GEOELECTRIC STRIKE)

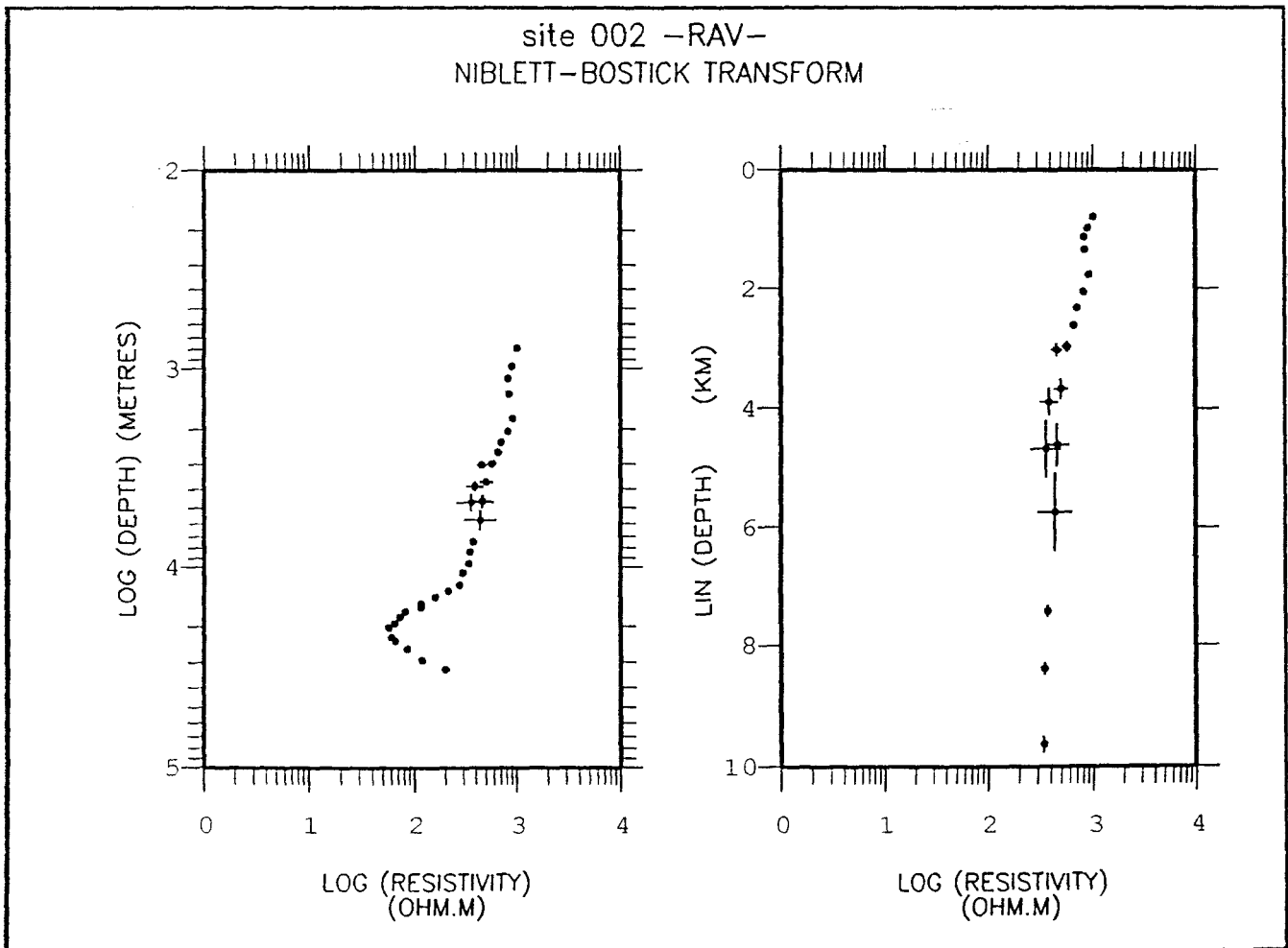
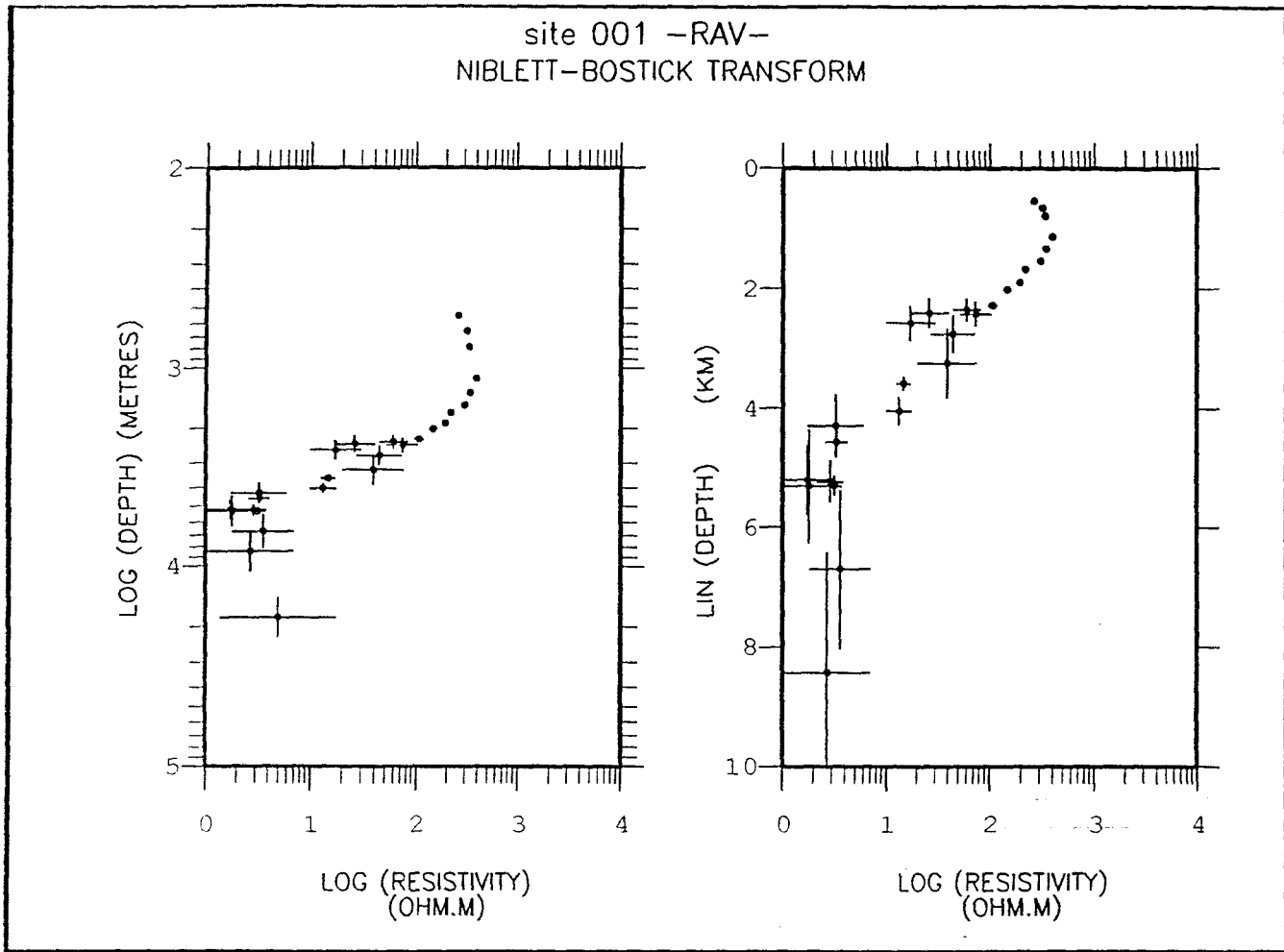


SITE 007 DIRECTION OF ANISOTROPY
(2-D GEOELECTRIC STRIKE)

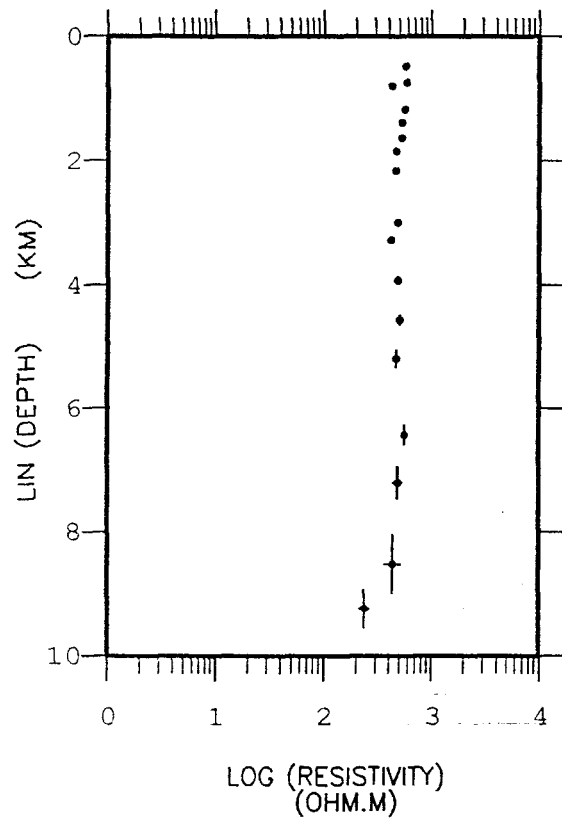
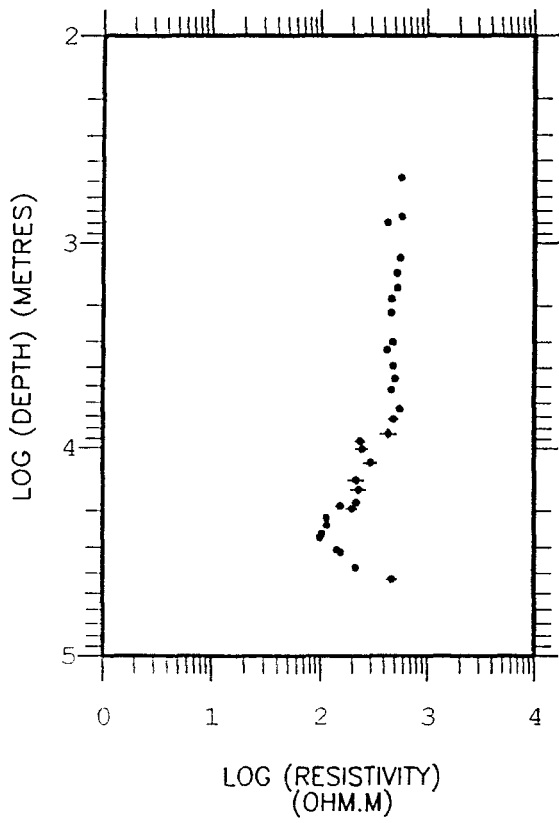


SITE 008 DIRECTION OF ANISOTROPY
(2-D GEOELECTRIC STRIKE)

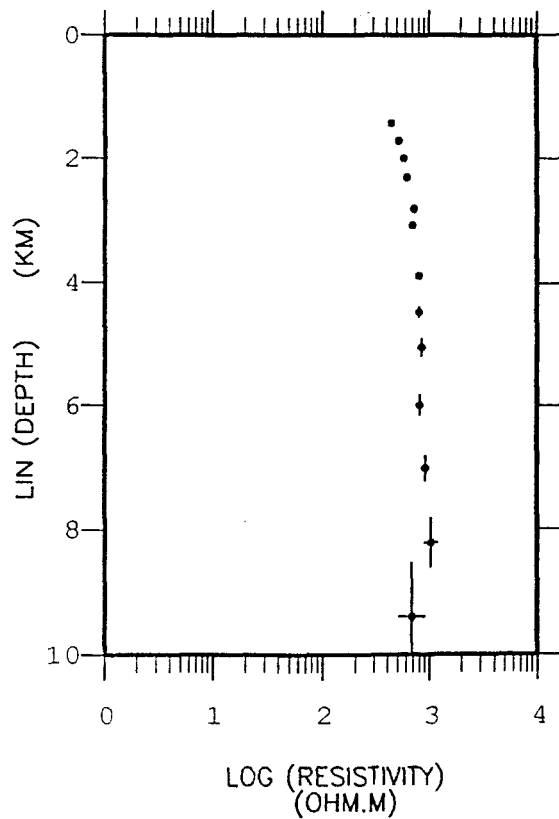
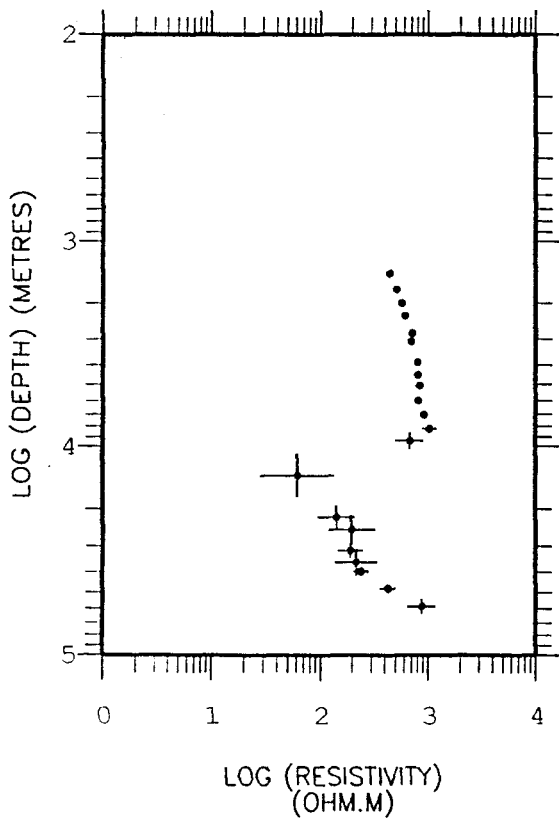




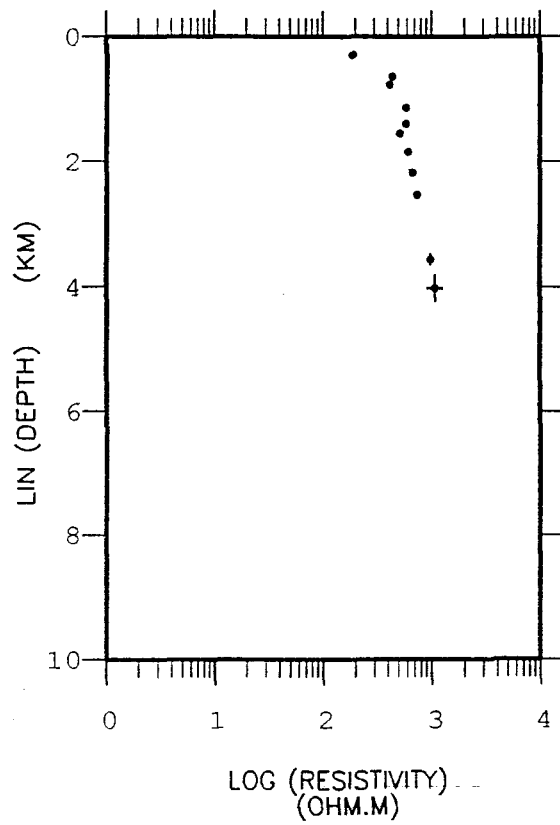
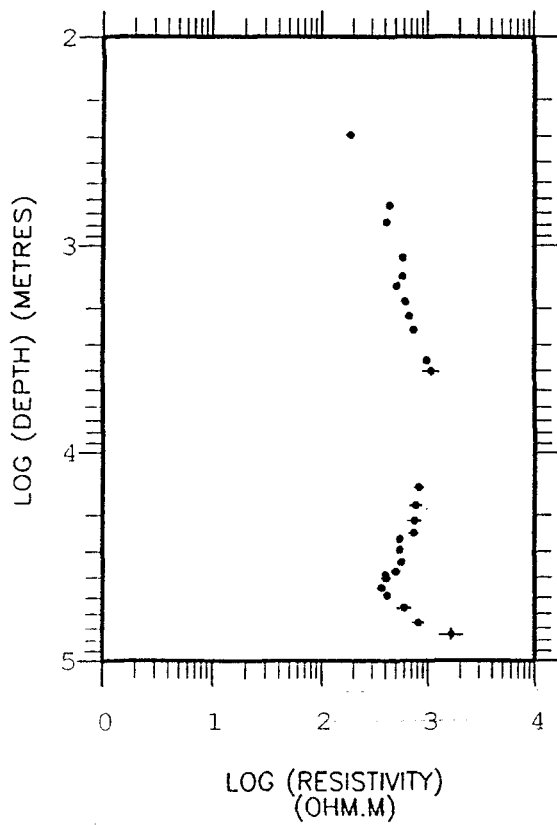
site 003 -RAV-
NIBLETT-BOSTICK TRANSFORM



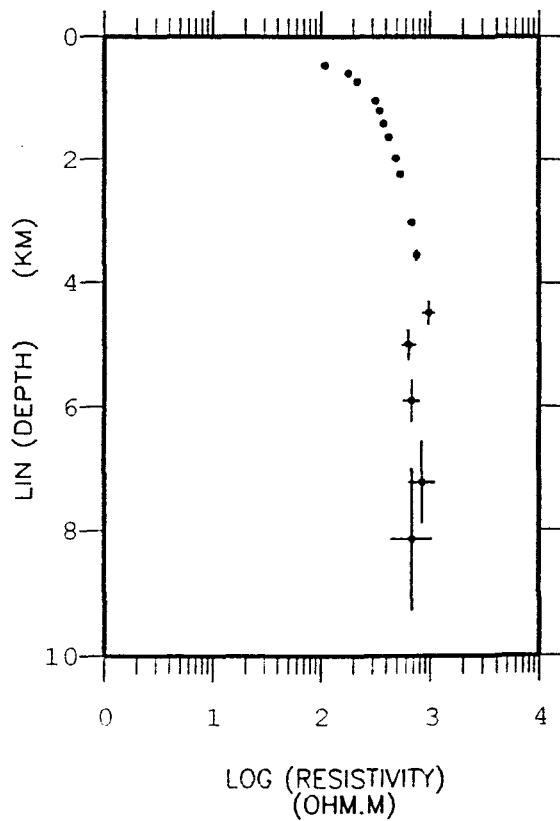
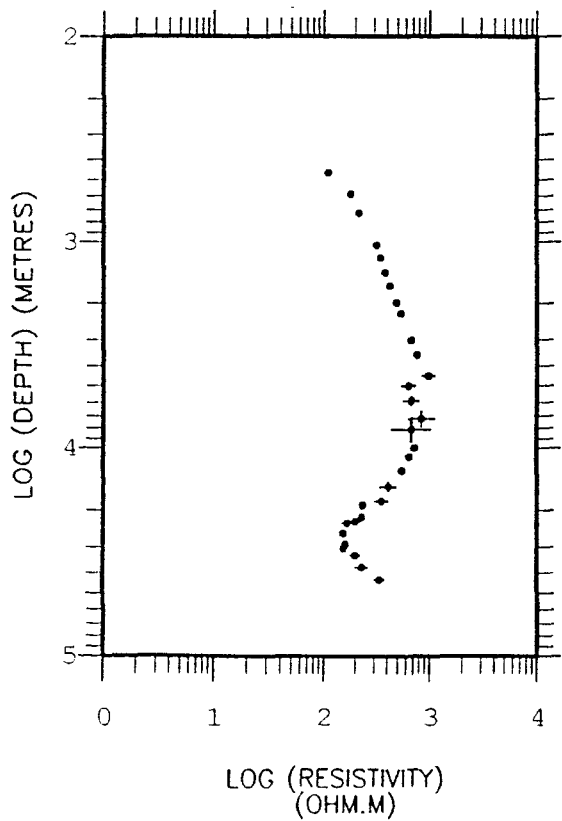
site 004 -RAV-
NIBLETT-BOSTICK TRANSFORM



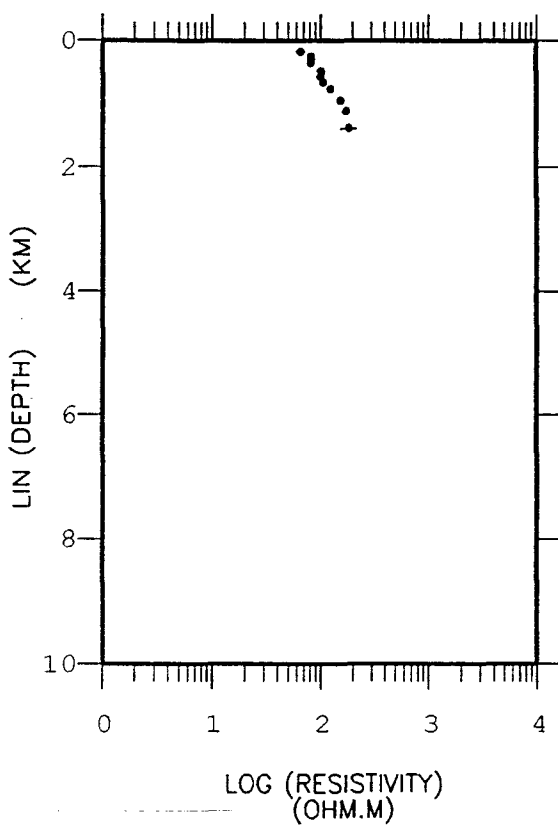
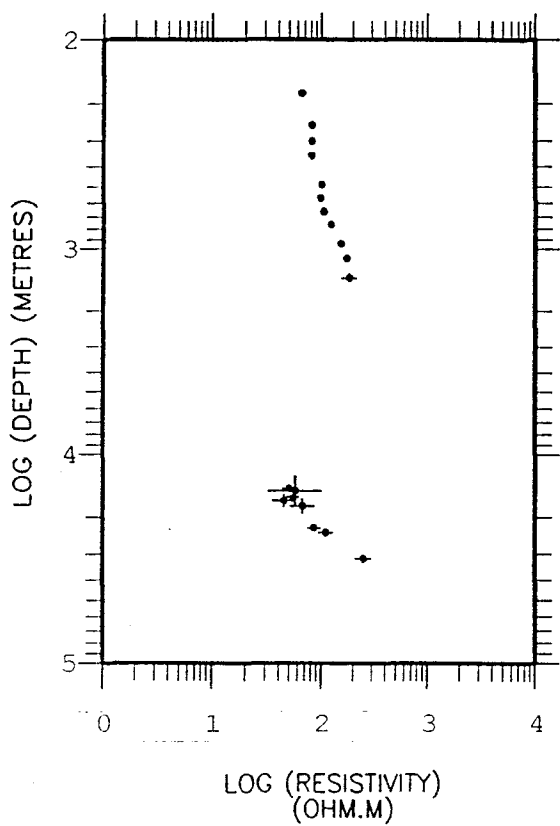
site 005 -RAV-
NIBLETT-BOSTICK TRANSFORM



site 006 -RAV-
NIBLETT-BOSTICK TRANSFORM



site 007 -RAV-
NIBLETT-BOSTICK TRANSFORM



site 008 -RAV-
NIBLETT-BOSTICK TRANSFORM

